Sex-specific modulation of the medial prefrontal cortex by glutamatergic median raphe neurons

Stuart A. Collins[1], Hannah E. Stinson[1], Amanda Himes[1], Andrea Nestor-Kalinoski[2]
Ipe Ninan[1*]

[1] Department of Neurosciences, University of Toledo College of Medicine and Life Sciences, Toledo, Ohio

[2] Department of Surgery, University of Toledo College of Medicine and Life Sciences, Toledo, Ohio

*Lead contact

Ipe Ninan, Department of Neurosciences, Department of Neurosciences, University of Toledo, Toledo, OH 43614

Email: Ipe.Ninan@utoledo.edu

Tel: 419 383 4126

Short title: Sex-specific role of median raphe VGLUT3 neurons

Summary

A substantial proportion of raphe neurons are glutamatergic. However, little is known about how these glutamatergic neurons modulate the forebrain. The present study investigated how glutamatergic median raphe nucleus (MRN) input modulates the medial prefrontal cortex (mPFC), a critical component of fear circuitry. Our studies show that VGLUT3-expressing MRN neurons activate VGLUT3- and somatostatin-expressing neurons in the mPFC. Consistent with this modulation of mPFC GABAergic neurons, activation of MRN (VGLUT3) neurons enhances GABAergic transmission in mPFC pyramidal neurons and attenuates fear memory in female but not male mice. In agreement with these female-specific effects, we observed sex differences in glutamatergic transmission onto MRN (VGLUT3) neurons and in mPFC (VGLUT3) neuron-mediated dual release of glutamate and GABA. Thus, our results demonstrate a cell type- and sex-specific modulation of the mPFC by MRN (VGLUT3) neurons.

INTRODUCTION

The medial prefrontal cortex (mPFC) plays a critical role in regulating fear memory [1]. While the dorsal mPFC (prelimbic, PL-mPFC) is involved in the expression of fear memory, the ventral mPFC (infralimbic, IL-mPFC) is important for fear extinction, an inhibitory mechanism that suppresses fear memory [1,2]. Although fear memory associated with a potential threat is necessary for survival, a diminished ability to regulate fear memory in a safe environment is implicated in anxiety and psychological trauma-related disorders [3-5]. Therefore, therapeutic interventions to attenuate fear memory might benefit the management of these disorders. An evidence-based approach to suppressing fear memory requires a better understanding of the neuromodulatory mechanisms in the fear circuitry. Activity in the median raphe nucleus (MRN), which projects to the mPFC, has been implicated in fear memory and anxiety-related behaviors [6-13]. However, the cellular specificity and synaptic mechanisms underlying the MRN modulation of the mPFC are unclear.

In addition to GABAergic and 5-HTergic neurons, the MRN contains neurons expressing vesicular glutamate transporters VGLUT2 and VGLUT3 [14-17]. Approximately 70% of MRN projections to the mPFC are VGLUT3-positive [10]. Despite the robust glutamatergic nature of the MRN input to the mPFC, activation of the MRN enhances inhibitory activity in the mPFC [18]. Therefore, it is possible that MRN (VGLUT3) neurons inhibit mPFC pyramidal neurons by activating local GABAergic neurons. A recent study showed that raphe neurons innervate GABAergic neurons in the mPFC [19]. This purported suppression of pyramidal neuron activity might affect fear memory. Using a cell-type specific expression of channelrhodopsin (ChR2), we show that MRN (VGLUT3) neurons modulate VGLUT3- and somatostatin (SST)-expressing neurons in the mPFC via glutamatergic transmission. Furthermore, activation of MRN (VGLUT3) axon terminals induces a long-lasting enhancement of GABAergic transmission in the female

mPFC. This activation of MRN (VGLUT3) axon terminals also suppresses excitatory synaptic transmission in the female PL-mPFC. Consistent with the sex difference in MRN (VGLUT3) neuron-mediated plasticity in the mPFC, chemogenetic activation of MRN (VGLUT3) neurons suppresses fear memory in female mice but not male mice. In agreement with these sex-specific effects in mPFC plasticity and fear memory suppression, we observed sex difference in glutamatergic input to MRN (VGLUT3) neurons and the synaptic output of mPFC (VGLUT3) neurons, a primary synaptic target of MRN (VGLUT3) neurons.

RESULTS

MRN (VGLUT3) neurons activate VGLUT3 and SST neurons in the mPFC

First, we determined whether MRN (VGLUT3) neurons innervate the mPFC in a cell type-specific manner. Recent studies show colocalization of VGLUT3-expressing raphe axonal boutons with cortical VGLUT3 neurons, most of which are cholecystokinin (CCK)-expressing GABAergic neurons that release both glutamate and GABA [20-23]. We examined MRN (VGLUT3) neuron-mediated transmission in mPFC (VGLUT3) neurons. Light-evoked currents were recorded at -60mV in tdTomato-expressing mPFC (VGLUT3) neurons from VGLUT3-tdTomato mice (generated by crossing B6;129S-*Slc17a8*$^{tm1.1(cre)Hze}$/J mice with B6.Cg-Gt(ROSA)26Sortm14(CAG-tdTomato)Hze/J mice) that received AAV-EF1a-double floxed-hChR2(H134R)-mCherry/EYFP-WPRE-HGHpA injection into the MRN. Of the 201 mPFC (VGLUT3) neurons (116 neurons from 11 female+85 neurons from 7 male mice) recorded, 21 (12 from female mice+9 from male mice) neurons showed synaptic currents in response to light activation of MRN (VGLUT3) terminals (mean amplitude: 28.16±10.09pA) (Figure 1B). We examined whether MRN (VGLUT3) neuron-mediated transmission in mPFC (VGLUT3) neurons is monosynaptic by studying the effect of 4-aminopyridine (4-AP, 100 μM), a blocker of voltage-

gated potassium channels, on tetrodotoxin (TTX, 1 μM)-induced suppression of light-evoked currents in mPFC (VGLUT3) neurons (Figure 1B) [24]. Only 4 neurons (from 2 female and 1 male mouse) out of 9 neurons (from 4 female and 4 male mice) showed 4-AP-induced rescue of EPSCs, suggesting that MRN (VGLUT3) neurons activate mPFC (VGLUT3) neurons via both monosynaptic and polysynaptic connections. The average delay between the onset of the light stimulus and synaptic currents before the application of TTX were 1.91±0.13ms and 8.21±0.4ms for monosynaptic (4-AP responsive) and polysynaptic (4-AP unresponsive) currents, respectively. The currents in the presence of both TTX and 4-AP were blocked by DNQX (10 μM), an AMPA receptor blocker, confirming the glutamatergic nature of this synaptic transmission (Figure 1B). Apart from MRN (VGLUT3) neuron-mediated glutamatergic transmission in mPFC (VGLUT3) neurons, we studied MRN (VGLUT3) neuron-mediated transmission in SST neurons in the mPFC. Light-evoked currents in EGFP-expressing SST neurons from MRN (VGLUT3)-ChR2-GIN mice were recorded. To generate MRN (VGLUT3)-ChR2-GIN mice, we first crossed B6;129S-*Slc17a8*$^{tm1.1(cre)Hze}$/J mice with FVB-Tg(GadGFP)45704Swn/J (GIN) mice [25,26]. Then, the progeny expressing both Cre and EGFP were injected with AAV-EF1a-double floxed-hChR2(H134R)-mCherry-WPRE-HGHpA into the MRN. We observed that 7 neurons (from 2 female and 5 male mice) out of 133 EGFP-expressing SST neurons (50 neurons/8 female mice+83 neurons/10 male mice) exhibited synaptic currents in response to a light activation (mean amplitude: 18±3.09pA) and that these currents were blocked by DNQX confirming the glutamatergic nature of this synaptic transmission (Figure 1C). The average delay between the onset of the light stimulus and synaptic response was 5.3±0.8ms, suggesting that the MRN (VGLUT3) neuron modulation of mPFC (SST) neurons is not monosynaptic. Consistently, bath application of 4-AP failed to rescue TTX-induced blockade of MRN (VGLUT3) neuron-mediated

currents in mPFC (SST) neurons (Figure 1C). In contrast to MRN (VGLUT3)-mediated synaptic transmission in SST and VGLUT3 neurons in the mPFC; we did not observe light-evoked synaptic responses in EGFP-expressing parvalbumin (PV) neurons (50 neurons/4 female+56 neurons/3male mice) of MRN (VGLUT3)-ChR2-G42 mice [mice expressing ChR2 in MRN (VGLUT3) neurons and EGFP in PV neurons] [27] (Figure 1D). MRN (VGLUT3)-ChR2-G42 mice were generated using the same breeding approach used for MRN (VGLUT3)-ChR2-GIN mice. Similar to the results in PV neurons, none of the recorded pyramidal neurons (146 neurons/31 female+137 neurons/27 male mice) showed a fast synaptic response to light stimulation (Figure 1D). These results suggest the possibility that MRN (VGLUT3) neurons enhance synaptic inhibition in the mPFC by activating VGLUT3 and SST neurons.

Activation of MRN (VGLUT3) axon terminals induces a long-lasting enhancement of GABAergic transmission in the PL-mPFC pyramidal neurons of female but not male mice

Based on our data showing MRN (VGLUT3) neuron-mediated glutamatergic currents in VGLUT3 and SST neurons in the mPFC, we asked whether activity in MRN (VGLUT3) axon terminals affects GABAergic transmission in layer 5 pyramidal neurons. To study the effect of light-induced activation of MRN (VGLUT3) axon terminals in the mPFC, we used MRN (VGLUT3)-ChR2 mice, as described above. As controls, we used MRN-EGFP mice, which received AAV-hSyn-EGFP injection into the MRN. MRN (VGLUT3) terminals were activated by a 10 Hz light stimulation for 60s (each pulse of 2ms duration). Spontaneous inhibitory post-synaptic currents (sIPSCs) were recorded at 0 mV before and after the 10 Hz stimulation. This 10 Hz stimulation produced a long-lasting enhancement of both the frequency and amplitude of sIPSCs in the PL-mPFC pyramidal neurons of female MRN (VGLUT3)-ChR2 mice but not MRN-EGFP mice (Figure 2A). However, this GABAergic plasticity in PL-mPFC pyramidal neurons was

absent in male MRN (VGLUT3)-ChR2 mice (Figure 2B). Consistently, statistical analysis shows a significant effect of sex and an interaction between treatment and sex on MRN (VGLUT3) neuron-mediated enhancement of sIPSC frequency but not amplitude in PL-mPFC pyramidal neurons.

Next, we examined whether a similar MRN (VGLUT3) neuron-mediated GABAergic plasticity occurs in the IL-mPFC. Although the 10 Hz light stimulation showed a late increase in sIPSC frequency in the female MRN (VGLUT3)-ChR2 group compared to the MRN-EGFP group, we did not observe any change in sIPSC amplitude in female mice after the 10Hz light stimulation (Figure 3A). We did not observe any change in sIPSC amplitude or frequency in the male MRN (VGLUT3)-ChR2 group compared to the MRN-EGFP group (Figure 3B). Statistical analysis did not show an effect of sex or an interaction between treatment and sex on MRN (VGLUT3) neuron-mediated GABAergic plasticity in IL-mPFC pyramidal neurons. These results show that activation of MRN (VGLUT3) terminals produces a sex- and region-specific GABAergic plasticity in mPFC pyramidal neurons.

Activation of MRN (VGLUT3) axon terminals suppresses excitatory synaptic transmission in the PL-mPFC pyramidal neurons of female but not male mice

Given the long-lasting enhancement of GABAergic transmission in the PL-mPFC pyramidal neurons of female mice following the activation of MRN (VGLUT3) terminals, we asked whether this activity affects excitatory synaptic transmission in mPFC pyramidal neurons. We measured excitatory post-synaptic potential (EPSP) slope in PL-mPFC and IL-mPFC layer 5 pyramidal neurons before and after a 10Hz light stimulation. We observed a long-lasting depression of EPSP slope in the PL-mPFC pyramidal neurons of female but not male MRN (VGLUT3)-ChR2 mice (Figures 4A,B). Consistently, statistical analysis shows a significant effect

of sex on changes in EPSP slope in the PL-mPFC. However, this 10Hz stimulation did not produce a statistically significant effect in female IL-mPFC pyramidal neurons (Figure 4C). Interestingly, we observed a delayed suppression of EPSP slope in male IL-mPFC pyramidal neurons (Figure 4D). These results suggest that MRN (VGLUT3) neuron activity suppresses mPFC excitatory synaptic activity in a region- and sex-specific manner.

Activation of MRN (VGLUT3) axon terminals does not affect the membrane properties of mPFC pyramidal neurons

Although the light activation of MRN (VGLUT3) terminals produced sex- and region-specific changes in GABAergic and glutamatergic transmission in the mPFC, our analysis of passive and active membrane properties in PL-mPFC and IL-mPFC layer 5 pyramidal neurons did not show an effect of MRN (VGLUT3) neuronal activity on input resistance, time constant, capacitance, resting membrane potential or frequency of action potentials evoked by current injection (Figures S1-S4). These results suggest that the activation of MRN (VGLUT3) neurons selectively affects the synaptic properties but not the membrane properties of mPFC pyramidal neurons.

The observed sex difference in the aforementioned synaptic changes is unlikely to be caused by sex differences in the MRN (VGLUT3) innervation of the mPFC as our comparison of MRN (VGLUT3) fiber density in the PL-mPFC from 3 female and 3 male VGLUT3-ChR2 mice did not show statistically significant sex difference (Figure S5).

Activation of MRN (VGLUT3) neurons suppresses fear memory in female but not male mice

Our results show that activity in MRN (VGLUT3) neurons produces a robust and long-lasting increase in GABAergic transmission and a suppression of excitatory synaptic transmission in the PL-mPFC of female mice. Given the involvement of the mPFC in regulating fear memory

and fear extinction, we examined whether activation of MRN (VGLUT3) neurons affects fear memory or extinction. We studied fear memory and extinction in mice expressing hM3D(Gq) in MRN (VGLUT3) neurons [MRN (VGLUT3)-hM3D(Gq) mice, B6;129S-*Slc17a8*$^{tm1.1(cre)Hze}$/J mice that received AAV-hSyn-DIO-hM3D(Gq)-mCherry injection into the MRN]. Mice were used 3 weeks after the surgery. On day 1 of the behavioral experiments, mice underwent fear conditioning. On day 2, the fear-conditioned mice received either saline or clozapine N-oxide (CNO, 1 mg/kg), followed by fear extinction training 1 hr later. On day 3, all mice were tested for extinction memory. We did not observe a difference in freezing between the CNO and saline groups on day 3 in both males and females (Figures 5C, D), suggesting a lack of effect of MRN (VGLUT3) neuron activation on fear extinction. However, a comparison of the first three trials during the extinction training on day 2 revealed that freezing is significantly lower in the female CNO group compared to the female saline group (Figure 5C). This effect of MRN (VGLUT3) neuron activation on fear memory was lacking in male mice (Figure 5D), suggesting that an activation of MRN (VGLUT3) neurons suppresses fear memory only in females. Although we did not observe an effect of sex on freezing during early extinction training, we observed a significant interaction between treatment and sex. In control experiments, CNO (1 mg/kg) did not affect fear memory or extinction in mice that received an AAV-hSyn-EGFP injection into the MRN, suggesting the absence of non-specific effects of CNO on fear memory or extinction (Figure S6).

Next, we tested whether suppression of activity in MRN (VGLUT3) neurons affects fear memory or extinction. We studied fear memory and extinction in mice expressing hM4D(Gi) in MRN (VGLUT3) neurons [MRN (VGLUT3)-hM4D(Gi) mice, B6;129S-*Slc17a8*$^{tm1.1(cre)Hze}$/J mice that received AAV-hSyn-DIO-hM4D(Gi) -mCherry injection into the MRN]. Neither female nor male mice showed an effect on fear memory or extinction after the chemogenetic suppression

of MRN (VGLUT3) neurons (Figures 5F, G). These results suggest that only an increase but not a decrease in the activity of MRN (VGLUT3) neurons affects fear memory in female mice.

Fear conditioning enhances glutamatergic transmission onto MRN (VGLUT3) neurons in female but not male mice

Since MRN (VGLUT3) neuronal activity affects PL-mPFC synaptic transmission and fear memory in female mice, we examined whether fear conditioning or extinction involves changes in synaptic transmission onto MRN (VGLUT3) neurons. We recorded spontaneous glutamatergic and GABAergic transmission in tdTomato-expressing MRN neurons from control tone-alone (TA), fear-conditioned (FC), and fear-extinguished (FE) VGLUT3-tdTomato mice. Miniature excitatory post-synaptic currents (mEPSCs) and miniature inhibitory post-synaptic currents (mIPSCs) were recorded in VGLUT3 neurons at -50 mV and 0 mV, respectively. Interestingly, we observed an enhanced mEPSC amplitude in the FC female group compared to the TA female group (Figure 6B). However, this increase in mEPSC amplitude was not associated with any significant change in mEPSC frequency. Furthermore, the mEPSC amplitude of the FC group was not significantly different from that of the FE group, suggesting that fear extinction does not reverse the fear conditioning-induced increase in AMPA receptor-mediated synaptic transmission in MRN (VGLUT3) neurons. Neither fear conditioning nor extinction affected mEPSCs in male mice (Figure 6C). A comparison of mIPSC frequency and amplitude among the TA, FC, and FE groups did not show a statistically significant effect in female or male mice (Figures 6B, C). Statistical analysis revealed an interaction between sex and treatment on mEPSC amplitude. These results indicate that fear conditioning involves an enhancement of glutamatergic but not GABAergic transmission in MRN (VGLUT3) neurons and that this experience-dependent plasticity occurs only in female mice.

Using the control TA groups, we also examined whether the basal glutamatergic or GABAergic transmission in MRN (VGLUT3) neurons exhibits a sex difference. Our analysis showed that the amplitude of mEPSCs is significantly higher in the male TA group compared to the female TA group. However, we did not observe a sex difference in mEPSC frequency, mIPSC amplitude, or mIPSC frequency in the TA groups. These results suggest a diminished basal AMPA receptor transmission in the MRN (VGLUT3) neurons of female mice.

We also compared the passive and active membrane properties of VGLUT3 neurons from the TA, FC, and FE groups. Although the female FC group showed an increase in action potentials, this effect did not reach statistical significance (Figure S7A). We did not observe a significant effect of fear conditioning or extinction on membrane properties in male mice (Figure S7B). Also, we did not observe any sex differences in basal passive and active membrane properties except that the female TA group showed a significant depolarization compared to the male TA group (figs. S7A,B).

These results suggest that MRN (VGLUT3) neurons in female mice exhibit a diminished glutamatergic input compared to those in male mice, while fear conditioning enhances glutamatergic transmission in the MRN (VGLUT3) neurons of female but not male mice. This sex difference in glutamatergic transmission and experience-dependent glutamatergic plasticity in MRN (VGLUT3) neurons might contribute to female-specific mPFC plasticity and fear memory suppression following the activation of MRN (VGLUT3) neurons.

PL-mPFC (VGLUT3) neuron-mediated synaptic transmission shows sex difference

Since the observed female-specific effect of MRN (VGLUT3) neuronal activation on PL-mPFC synaptic plasticity and fear memory could also involve sex-specific effects within the PL-mPFC, we asked whether PL-mPFC (VGLUT3) neurons modulate other mPFC neurons in a sex-

specific manner. We recorded PL-mPFC (VGLUT3) neuron-mediated EPSCs and IPSCs at -20 mV in EGFP-expressing SST neurons and pyramidal neurons from PL-mPFC (VGLUT3)-ChR2-GIN mice, which were generated by injecting AAV-EF1a-double floxed-hChR2(H134R)-mCherry-WPRE-HGHpA into the PL-mPFC of *Slc17a8*$^{tm1.1(cre)Hze}$/J mice crossed with GIN mice. First, we confirmed that PL-mPFC (VGLUT3) neuron-mediated inward currents (EPSCs) in SST neurons are blocked by DNQX, an AMPA receptor antagonist. To understand whether these EPSCs are monosynaptic, we studied the effect of 4-AP on the TTX block of inward currents. 4-AP rescued EPSCs in all 6 cells tested. Therefore, PL-mPFC (VGLUT3) neuron-mediated EPSCs in SST neurons are predominantly monosynaptic. The average EPSC amplitudes calculated before any drug application were significantly higher in female mice than in male mice (Figure 7B). 4-AP rescued TTX-induced block of IPSCs in only 2 out of 5 cells tested. These results suggest that PL-mPFC (VGLUT3) neuron-mediated IPSCs in SST neurons are mediated by both monosynaptic and disynaptic transmission. The 4-AP rescue experiments in neurons which showed monosynaptic EPSCs and IPSCs required a blockade of EPSCs with AMPA and NMDA receptor antagonists to reveal the rescued IPSC (example traces, Figure 7B). Similar to EPSC amplitudes, the average IPSC amplitudes calculated before any drug application were significantly higher in female mice than in male mice (Figure 7B). We measured the excitatory/inhibitory balance of PL-mPFC (VGLUT3) neuron-mediated transmission in SST neurons by calculating the ratio of EPSC amplitude to IPSC amplitude at a single neuron level (E/I ratio). We did not observe a sex difference in the E/I ratio, suggesting that the overall PL-mPFC (VGLUT3) neuron-mediated transmission in SST neurons is higher in female mice (Figure 7B).

DNQX blocked PL-mPFC (VGLUT3) neuron-mediated EPSCs in pyramidal neurons. 4-AP rescued TTX-induced block of EPSCs in all 6 cells tested, suggesting a predominant

monosynaptic PL-mPFC (VGLUT3) neuron-pyramidal neuron glutamatergic transmission. Unlike the SST neurons, we did not observe any sex difference in mPFC (VGLUT3) neuron-mediated EPSC amplitude in pyramidal neurons (Figure 7C). 4-AP rescued TTX-induced block of IPSCs in only 2 out of 6 cells tested. These results suggest that PL-mPFC (VGLUT3) neuron-mediated IPSCs in pyramidal neurons are mediated by both monosynaptic and disynaptic transmission. Similar to 4-AP rescue experiments in SST neurons, a blockade of the AMPA and NMDA receptors was necessary to reveal the rescued IPSC in pyramidal neurons, which showed monosynaptic EPSCs and IPSCs (example traces, Figure 7C). Similar to EPSC amplitudes, we did not observe any sex difference in mPFC (VGLUT3) neuron-mediated IPSC amplitude in pyramidal neurons. (Figure 7C). However, a decreased E/I ratio in female mice compared to male mice suggested that the PL-mPFC (VGLUT3) neuron-mediated inhibition of pyramidal neurons at the single neuron level is higher in female mice (Figure 7C). We also examined PL-mPFC (VGLUT3) neuron-mediated glutamatergic and GABAergic transmission in local PV neurons. Measurement of EPSCs (18.9±8.4pA) and IPSCs (29.2±20.5pA) in EGFP-expressing PV neurons from PL-mPFC (VGLUT3)-ChR2-G42 mice (Figure S8) showed that PL-mPFC (VGLUT3) neuron-mediated transmission in local PV neurons is weaker than that in SST neurons (EPSC=35.2±6.6pA, IPSC=67.07.6±16.24pA) (Figure 7B) and pyramidal neurons (EPSC=60.9±14.9pA, IPSC=101.3±26.7pA) (Figure 7C). We did not observe sex difference in EPSC amplitude, IPSC amplitude, or E/I ratio in PV neurons. These results suggest that the sex difference in PL-mPFC (VGLUT3) neuron-mediated transmission in local SST and pyramidal neurons might contribute to the sex-specific effect of MRN (VGLUT3) neuronal activation on PL-mPFC synaptic plasticity and fear memory suppression.

DISCUSSION

Our studies show MRN (VGLUT3) neuron-mediated monosynaptic activation of mPFC (VGLUT3) neurons. The MRN (VGLUT3) neuron-mediated polysynaptic responses in mPFC VGLUT3 and SST neurons but not in PV or pyramidal neurons suggest the possibility that MRN (VGLUT3) neurons preferentially innervate mPFC (VGLUT3) neurons that form synapses onto local SST neurons and VGLUT3 neurons. Consistent with MRN (VGLUT3) neuron-mediated excitatory responses in these mPFC GABAergic neurons, activation of MRN (VGLUT3) terminals produced a long-lasting enhancement of GABAergic transmission and a long-lasting depression of excitatory synaptic transmission in PL-mPFC pyramidal neurons from female but not male mice. In agreement with MRN (VGLUT3) neuron-mediated plasticity in the PL-mPFC, we observed a suppression of fear memory in female but not male mice following the chemogenetic activation of MRN (VGLUT3) neurons. These results are significant given the role of the PL-mPFC in fear memory expression [1,28,29].

MRN neurons are functionally heterogeneous. In addition to GABAergic neurons, the MRN contains neurons expressing VGLUT2, VGLUT3, and 5-HT [14-17]. Most MRN neurons projecting to the mPFC are VGLUT3-expressing neurons [10]. An earlier study showed that raphe serotonergic neurons activate mPFC GABAergic neurons by releasing glutamate [19]. Also, the VGLUT3-expressing raphe axons co-localize with cortical VGLUT3 neurons [23]. Our experiments demonstrate that MRN (VGLUT3) neurons activate VGLUT3 and SST neurons in the mPFC. This neuromodulation is particularly significant as the dual release of glutamate and GABA from mPFC (VGLUT3) neurons and SST neuron-mediated GABA release affect pyramidal neuron activity [30-32]. Therefore, MRN (VGLUT3) neuron-mediated activation of mPFC VGLUT3 and SST neurons

and the resulting GABAergic inhibition of mPFC pyramidal neurons might play a role in the suppression of fear memory in female mice.

The female-specific mPFC plasticity and fear memory suppression might be due to a combined effect of multiple synapses along the MRN (VGLUT3)-mPFC pathway. The basal glutamatergic but not GABAergic transmission in MRN (VGLUT3) neurons is diminished in female mice compared to male mice. Furthermore, fear conditioning involves an enhanced glutamatergic transmission in the MRN (VGLUT3) neurons of female mice but not male mice. A diminished basal glutamatergic transmission in MRN (VGLUT3) neurons and its potentiation in response to fear conditioning might be a critical mechanism for MRN (VGLUT3)-mediated suppression of fear memory in female mice. This experience-dependent glutamatergic plasticity might make MRN (VGLUT3) neurons more amenable to chemogenetic activation, leading to an attenuation of PL-mPFC function and hence the suppression of fear memory in female mice. Also, the higher basal glutamatergic transmission in MRN (VGLUT3) neurons in male mice might result in an increased bottom-up modulation of the mPFC, and this effect might occlude the impact of chemogenetic activation. The diminished glutamatergic drive onto MRN (VGLUT3) neurons in female mice compared to male mice could contribute to the sex difference in behaviors relevant to anxiety- or psychological trauma-related disorders [33-35].

In addition to the sex difference in glutamatergic transmission and plasticity in MRN (VGLUT3) neurons, the PL-mPFC (VGLUT3)-SST neuron transmission is significantly higher in females compared to males. Also, the E/I ratio of the PL-mPFC (VGLUT3) neuron-pyramidal neuron transmission in female mice is lower than that of male mice. Given that MRN (VGLUT3) neurons primarily target VGLUT3 neurons in the mPFC, sex difference in PL-mPFC (VGLUT3) neuron-mediated transmission in local SST and pyramidal neurons might be an additional

mechanism that augments the effect of MRN (VGLUT3) neuron-mediated inhibition of PL-mPFC pyramidal neurons in female mice. Thus, the sex difference in both the synaptic transmission in MRN (VGLUT3) neurons and the synaptic output of PL-mPFC (VGLUT3) neurons might play a key role in female-specific synaptic plasticity in the PL-mPFC and fear memory suppression following the activation of MRN (VGLUT3) neurons. Chromosomal and hormonal effects might play a role in establishing these sex-specific circuits [36].

In conclusion, our study demonstrates that MRN (VGLUT3) neurons modulate the mPFC through glutamatergic transmission in VGLUT3 and SST GABAergic neurons. Furthermore, this study describes sex-specific synaptic transmission and plasticity in the MRN (VGLUT3)-mPFC neuromodulatory pathway and their potential role in suppressing fear memory in female mice. Given the increased prevalence of anxiety- and psychological trauma-related disorders in females compared to males, identifying synaptic and molecular targets in this neuromodulatory pathway that are responsive to pharmacological or behavioral interventions might provide critical insights into evidence-based approaches to managing psychiatric disorders.

Limitations of the study

A limitation of our study is the need for experiments to demonstrate the causal role of the PL-mPFC in MRN (VGLUT3)-mediated suppression of fear memory. Given the MRN (VGLUT3) inputs in the hippocampus and the medial septum, these brain areas also might play a role in the behavioral effects of MRN (VGLUT3) neuron activation [10,37-39]. Therefore, future studies will be necessary to dissect the specific roles of these target brain areas in mediating the effect of MRN (VGLUT3) neurons on behavior. Also, future research will be necessary to understand the role of 5-HT3a receptor-expressing non-VGLUT3 neurons in MRN (VGLUT3) neuron-mediated effects in the mPFC [40].

Acknowledgments

AAV-EF1a-double floxed-hChR2(H134R)-mCherry-WPRE-HGHpA (20297-AAV9, Addgene) and AAV-EF1a-double floxed-hChR2(H134R)-EYFP-WPRE-HGHpA (20298-AAV9, Addgene) were gifts from Dr. Karl Deisseroth. AAV-hSyn-EGFP (50465-AAV2, Addgene), AAV-hSyn-DIO-EGFP (50457-AAV2, Addgene), AAV-hSyn-DIO-hM4D(Gi)-mCherry (44362-AAV2, Addgene) and AAV-hSyn-DIO-hM3D(Gq)-mCherry (44361-AAV2, Addgene) were gifts from Dr. Bryan Roth. We thank Dr. Peter Koppensteiner for his comments on the manuscript. This work was supported by the National Institutes of Health (grant number HD076914 to I.N.).

Author Contributions

Conceptualization: SAC, IN, Methodology: SAC, HES, ANK, IN, Investigation: SAC, HES, AH, ANK, IN, Supervision: ANK, IN, Writing: IN, Writing-review & editing: SAC, HES, ANK, IN

Declaration of interests

The authors declare no competing interest.

References

1. Corcoran, K.A., and Quirk, G.J. (2007). Activity in prelimbic cortex is necessary for the expression of learned, but not innate, fears. J Neurosci *27*, 840-844.
2. Milad, M.R., and Quirk, G.J. (2002). Neurons in medial prefrontal cortex signal memory for fear extinction. Nature *420*, 70-74.
3. Graham, B.M., and Milad, M.R. (2011). The study of fear extinction: implications for anxiety disorders. Am J Psychiatry *168*, 1255-1265. 10.1176/appi.ajp.2011.11040557 appi.ajp.2011.11040557 [pii].
4. Guthrie, R.M., and Bryant, R.A. (2006). Extinction learning before trauma and subsequent posttraumatic stress. Psychosom Med *68*, 307-311. 10.1097/01.psy.0000208629.67653.cc.
5. Wicking, M., Steiger, F., Nees, F., Diener, S.J., Grimm, O., Ruttorf, M., Schad, L.R., Winkelmann, T., Wirtz, G., and Flor, H. (2016). Deficient fear extinction memory in posttraumatic stress disorder. Neurobiol Learn Mem *136*, 116-126. 10.1016/j.nlm.2016.09.016.
6. Balazsfi, D.G., Zelena, D., Farkas, L., Demeter, K., Barna, I., Cserep, C., Takacs, V.T., Nyiri, G., Goloncser, F., Sperlagh, B., et al. (2017). Median raphe region stimulation alone generates remote, but not recent fear memory traces. PLoS One *12*, e0181264. 10.1371/journal.pone.0181264.
7. Avanzi, V., Castilho, V.M., de Andrade, T.G., and Brandao, M.L. (1998). Regulation of contextual conditioning by the median raphe nucleus. Brain Res *790*, 178-184. 10.1016/s0006-8993(97)01538-2.
8. Andrade, T.G., Zangrossi, H., Jr., and Graeff, F.G. (2013). The median raphe nucleus in anxiety revisited. Journal of psychopharmacology (Oxford, England) *27*, 1107-1115. 10.1177/0269881113499208.
9. Almada, R.C., Borelli, K.G., Albrechet-Souza, L., and Brandão, M.L. (2009). Serotonergic mechanisms of the median raphe nucleus-dorsal hippocampus in conditioned fear: Output circuit involves the prefrontal cortex and amygdala. Behavioural brain research *203*, 279-287. 10.1016/j.bbr.2009.05.017.
10. Szonyi, A., Mayer, M.I., Cserep, C., Takacs, V.T., Watanabe, M., Freund, T.F., and Nyiri, G. (2016). The ascending median raphe projections are mainly glutamatergic in the mouse forebrain. Brain Struct Funct *221*, 735-751. 10.1007/s00429-014-0935-1.
11. Meloni, E.G., Reedy, C.L., Cohen, B.M., and Carlezon, W.A., Jr. (2008). Activation of raphe efferents to the medial prefrontal cortex by corticotropin-releasing factor: correlation with anxiety-like behavior. Biological psychiatry *63*, 832-839. 10.1016/j.biopsych.2007.10.016.
12. Vertes, R.P., Fortin, W.J., and Crane, A.M. (1999). Projections of the median raphe nucleus in the rat. The Journal of comparative neurology *407*, 555-582.
13. Teissier, A., Chemiakine, A., Inbar, B., Bagchi, S., Ray, R.S., Palmiter, R.D., Dymecki, S.M., Moore, H., and Ansorge, M.S. (2015). Activity of Raphé Serotonergic Neurons Controls Emotional Behaviors. Cell Rep *13*, 1965-1976. 10.1016/j.celrep.2015.10.061.
14. Sos, K.E., Mayer, M.I., Cserep, C., Takacs, F.S., Szonyi, A., Freund, T.F., and Nyiri, G. (2017). Cellular architecture and transmitter phenotypes of neurons of the mouse median raphe region. Brain Struct Funct *222*, 287-299. 10.1007/s00429-016-1217-x.
15. Szőnyi, A., Zichó, K., Barth, A.M., Gönczi, R.T., Schlingloff, D., Török, B., Sipos, E., Major, A., Bardóczi, Z., Sos, K.E., et al. (2019). Median raphe controls acquisition of

negative experience in the mouse. Science (New York, N.Y.) *366*, eaay8746. 10.1126/science.aay8746.
16. Okaty, B.W., Commons, K.G., and Dymecki, S.M. (2019). Embracing diversity in the 5-HT neuronal system. Nature reviews. Neuroscience *20*, 397-424. 10.1038/s41583-019-0151-3.
17. Gras, C., Herzog, E., Bellenchi, G.C., Bernard, V., Ravassard, P., Pohl, M., Gasnier, B., Giros, B., and El Mestikawy, S. (2002). A third vesicular glutamate transporter expressed by cholinergic and serotoninergic neurons. The Journal of neuroscience : the official journal of the Society for Neuroscience *22*, 5442-5451. 10.1523/JNEUROSCI.22-13-05442.2002.
18. Hajós, M., Gartside, S.E., Varga, V., and Sharp, T. (2003). In vivo inhibition of neuronal activity in the rat ventromedial prefrontal cortex by midbrain-raphe nuclei: role of 5-HT1A receptors. Neuropharmacology *45*, 72-81. 10.1016/s0028-3908(03)00139-4.
19. Sun, Q., Li, X., Ren, M., Zhao, M., Zhong, Q., Ren, Y., Luo, P., Ni, H., Zhang, X., Zhang, C., et al. (2019). A whole-brain map of long-range inputs to GABAergic interneurons in the mouse medial prefrontal cortex. Nat Neurosci *22*, 1357-1370. 10.1038/s41593-019-0429-9.
20. Somogyi, J., Baude, A., Omori, Y., Shimizu, H., El Mestikawy, S., Fukaya, M., Shigemoto, R., Watanabe, M., and Somogyi, P. (2004). GABAergic basket cells expressing cholecystokinin contain vesicular glutamate transporter type 3 (VGLUT3) in their synaptic terminals in hippocampus and isocortex of the rat. Eur J Neurosci *19*, 552-569. 10.1111/j.0953-816x.2003.03091.x.
21. Fasano, C., Rocchetti, J., Pietrajtis, K., Zander, J.F., Manseau, F., Sakae, D.Y., Marcus-Sells, M., Ramet, L., Morel, L.J., Carrel, D., et al. (2017). Regulation of the Hippocampal Network by VGLUT3-Positive CCK- GABAergic Basket Cells. Front Cell Neurosci *11*, 140. 10.3389/fncel.2017.00140.
22. Pelkey, K.A., Calvigioni, D., Fang, C., Vargish, G., Ekins, T., Auville, K., Wester, J.C., Lai, M., Mackenzie-Gray Scott, C., Yuan, X., et al. (2020). Paradoxical network excitation by glutamate release from VGluT3(+) GABAergic interneurons. Elife *9*. 10.7554/eLife.51996.
23. Senft, R.A., Freret, M.E., Sturrock, N., and Dymecki, S.M. (2021). Neurochemically and Hodologically Distinct Ascending VGLUT3 versus Serotonin Subsystems Comprise the r2-Pet1 Median Raphe. J Neurosci *41*, 2581-2600. 10.1523/jneurosci.1667-20.2021.
24. Petreanu, L., Mao, T., Sternson, S.M., and Svoboda, K. (2009). The subcellular organization of neocortical excitatory connections. Nature *457*, 1142-1145. 10.1038/nature07709.
25. Oliva, A.A., Jr., Jiang, M., Lam, T., Smith, K.L., and Swann, J.W. (2000). Novel hippocampal interneuronal subtypes identified using transgenic mice that express green fluorescent protein in GABAergic interneurons. The Journal of neuroscience : the official journal of the Society for Neuroscience *20*, 3354-3368. 10.1523/JNEUROSCI.20-09-03354.2000.
26. Daigle, T.L., Madisen, L., Hage, T.A., Valley, M.T., Knoblich, U., Larsen, R.S., Takeno, M.M., Huang, L., Gu, H., Larsen, R., et al. (2018). A Suite of Transgenic Driver and Reporter Mouse Lines with Enhanced Brain-Cell-Type Targeting and Functionality. Cell *174*, 465-480.e422. 10.1016/j.cell.2018.06.035.

27. Chattopadhyaya, B., Di Cristo, G., Higashiyama, H., Knott, G.W., Kuhlman, S.J., Welker, E., and Huang, Z.J. (2004). Experience and activity-dependent maturation of perisomatic GABAergic innervation in primary visual cortex during a postnatal critical period. J Neurosci *24*, 9598-9611. 24/43/9598 [pii]
10.1523/JNEUROSCI.1851-04.2004.
28. Vidal-Gonzalez, I., Vidal-Gonzalez, B., Rauch, S.L., and Quirk, G.J. (2006). Microstimulation reveals opposing influences of prelimbic and infralimbic cortex on the expression of conditioned fear. Learn Mem *13*, 728-733. 13/6/728 [pii]
10.1101/lm.306106.
29. Giustino, T.F., and Maren, S. (2015). The Role of the Medial Prefrontal Cortex in the Conditioning and Extinction of Fear. Front Behav Neurosci *9*, 298. 10.3389/fnbeh.2015.00298.
30. Adler, A., Zhao, R., Shin, M.E., Yasuda, R., and Gan, W.B. (2019). Somatostatin-Expressing Interneurons Enable and Maintain Learning-Dependent Sequential Activation of Pyramidal Neurons. Neuron *102*, 202-216.e207. 10.1016/j.neuron.2019.01.036.
31. Koppensteiner, P., Von Itter, R., Melani, R., Galvin, C., Lee, F.S., and Ninan, I. (2019). Diminished Fear Extinction in Adolescents Is Associated With an Altered Somatostatin Interneuron-Mediated Inhibition in the Infralimbic Cortex. Biol Psychiatry *86*, 682-692. 10.1016/j.biopsych.2019.04.035.
32. Urban-Ciecko, J., Fanselow, E.E., and Barth, A.L. (2015). Neocortical somatostatin neurons reversibly silence excitatory transmission via GABAb receptors. Curr Biol *25*, 722-731. 10.1016/j.cub.2015.01.035.
33. Fenton, G.E., Halliday, D.M., Mason, R., Bredy, T.W., and Stevenson, C.W. (2016). Sex differences in learned fear expression and extinction involve altered gamma oscillations in medial prefrontal cortex. Neurobiol Learn Mem *135*, 66-72. 10.1016/j.nlm.2016.06.019.
34. Börchers, S., Krieger, J.P., Asker, M., Maric, I., and Skibicka, K.P. (2022). Commonly-used rodent tests of anxiety-like behavior lack predictive validity for human sex differences. Psychoneuroendocrinology *141*, 105733. 10.1016/j.psyneuen.2022.105733.
35. Botterill, J.J., Vinod, K.Y., Gerencer, K.J., Teixeira, C.M., LaFrancois, J.J., and Scharfman, H.E. (2021). Bidirectional Regulation of Cognitive and Anxiety-like Behaviors by Dentate Gyrus Mossy Cells in Male and Female Mice. J Neurosci *41*, 2475-2495. 10.1523/jneurosci.1724-20.2021.
36. Lentini, E., Kasahara, M., Arver, S., and Savic, I. (2013). Sex differences in the human brain and the impact of sex chromosomes and sex hormones. Cereb Cortex *23*, 2322-2336. 10.1093/cercor/bhs222.
37. Varga, V., Losonczy, A., Zemelman, B.V., Borhegyi, Z., Nyiri, G., Domonkos, A., Hangya, B., Holderith, N., Magee, J.C., and Freund, T.F. (2009). Fast synaptic subcortical control of hippocampal circuits. Science *326*, 449-453. 10.1126/science.1178307.
38. Jackson, J., Bland, B.H., and Antle, M.C. (2009). Nonserotonergic projection neurons in the midbrain raphe nuclei contain the vesicular glutamate transporter VGLUT3. Synapse (New York, N.Y.) *63*, 31-41. 10.1002/syn.20581.
39. Fortin-Houde, J., Henderson, F., Dumas, S., Ducharme, G., and Amilhon, B. (2023). Parallel streams of raphe VGLUT3-positive inputs target the dorsal and ventral hippocampus in each hemisphere. J Comp Neurol *531*, 702-719. 10.1002/cne.25452.

40. Huang, Z.J., and Paul, A. (2019). The diversity of GABAergic neurons and neural communication elements. Nat Rev Neurosci *20*, 563-572. 10.1038/s41583-019-0195-4.
41. Oliva, A.A., Jr., Jiang, M., Lam, T., Smith, K.L., and Swann, J.W. (2000). Novel hippocampal interneuronal subtypes identified using transgenic mice that express green fluorescent protein in GABAergic interneurons. J Neurosci *20*, 3354-3368.
42. Madisen, L., Zwingman, T.A., Sunkin, S.M., Oh, S.W., Zariwala, H.A., Gu, H., Ng, L.L., Palmiter, R.D., Hawrylycz, M.J., Jones, A.R., et al. (2010). A robust and high-throughput Cre reporting and characterization system for the whole mouse brain. Nat Neurosci *13*, 133-140. 10.1038/nn.2467.
43. Falcy, B.A., Mohr, M.A., and Micevych, P.E. (2020). Immunohistochemical amplification of mCherry fusion protein is necessary for proper visualization. MethodsX *7*, 100946. 10.1016/j.mex.2020.100946.
44. Grider, M.H., Chen, Q., and Shine, H.D. (2006). Semi-automated quantification of axonal densities in labeled CNS tissue. J Neurosci Methods *155*, 172-179. 10.1016/j.jneumeth.2005.12.021.
45. Collins, S.A., Ninan, I. (2021). Development-dependent plasticity in vasoactive intestinal polypeptide neurons in the infralimbic cortex. Cerebral Cortex Communications *2*, tgab007.
46. Koppensteiner, P., Galvin, C., and Ninan, I. (2019). Lack of experience-dependent intrinsic plasticity in the adolescent infralimbic medial prefrontal cortex. Synapse *73*, e22090. 10.1002/syn.22090.

Figure Legends

Figure 1. MRN (VGLUT3) neurons activate VGLUT3 and SST neurons in the mPFC.

A) Stereotactic injection of AAV-EF1a-double floxed-hChR2(H134R)-mCherry-WPRE-HGHpA into the MRN of VGLUT3 Cre mice. The left panel shows an example of mCherry-expressing MRN (VGLUT3) neurons. Scale: 100 μM. The right panel shows a schematic of mPFC slice preparation and whole-cell recording of mPFC neurons. **B**) The left panel is an example image showing EGFP-expressing mPFC (VGLUT3) neurons and MRN (VGLUT3) axons from a VGLUT3 Cre mouse injected with AAV-hSyn-DIO-EGFP into the mPFC and AAV-EF1a-double floxed-hChR2(H134R)-mCherry-WPRE-HGHpA into the MRN. Scale: 25 μM. Traces in the top middle panel demonstrate monosynaptic MRN (VGLUT3)-mPFC (VGLUT3) glutamatergic transmission. 4-AP (100 μM) rescued TTX (1 μM)-induced suppression of light-evoked currents. DNQX (10 μM), an AMPA receptor antagonist, blocked MRN (VGLUT3) neuron-mediated currents in mPFC (VGLUT3) neurons. Scale: 10 ms/50 pA. The right panel shows the mean EPSC amplitude in 4 mPFC (VGLUT3) neurons before TTX (control), in the presence of TTX, and TTX+4-AP. Traces in the lower panel show an example of polysynaptic MRN (VGLUT3) neuron-mediated transmission in mPFC (VGLUT3) neurons. Scale: 10 ms/25 pA. **C**) The left panel is an example image showing an EGFP-expressing mPFC (SST) neuron and mCherry-expressing MRN (VGLUT3) axons. Scale: 10 μM. Traces in the middle panel show MRN (VGLUT3) neuron-mediated glutamatergic current in an mPFC (SST) neuron. Scale: 10 ms/10 pA. Traces in the right panel show an example of polysynaptic MRN (VGLUT3) neuron-mediated transmission in mPFC (SST) neurons. Scale: 10 ms/50 pA. **D**) Summary of results from experiments to examine MRN (VGLUT3) neuron-mediated transmission in SST (N = 58 X PL-mPFC, 75 X IL-mPFC), PV (N

= 48 X PL-mPFC, 58 X IL-mPFC), VGLUT3 (N = 201 X PL-mPFC), and pyramidal neurons (N = 215 X PL-mPFC, 68 X IL-mPFC). Blue lines indicate the application of light (470 nm).

Figure 2. Activation of MRN (VGLUT3) axon terminals enhances GABAergic transmission in the PL-mPFC pyramidal neurons of female but not male mice.

A) The upper panel shows a schematic of whole-cell recording of pyramidal neurons and the application of 10Hz light stimulation to activate MRN (VGLUT3) terminals. A 10 Hz light stimulation for 60s enhanced sIPSC frequency ($F_{1,17}$=16.9, P<0.001) and amplitude ($F_{1,17}$=4.7, P=0.046) in PL-mPFC pyramidal neurons from female MRN (VGLUT3)-ChR2 group (10 neurons/5 mice) compared to MRN-EGFP group (9 neurons/5 mice). **B**) PL-mPFC pyramidal neurons in male MRN (VGLUT3)-ChR2 group (9 neurons/5 mice) did not show a significant change in either frequency ($F_{1,16}$=0.05, P=0.83) or amplitude ($F_{1,16}$=0.08, P=0.77) of sIPSCs as compared to MRN-EGFP group (9 neurons/5 mice). The upper panel shows example traces. Scale: 100 pA/250 ms. A two-way ANOVA showed a significant effect of sex ($F_{3,36}$=27.75, P=0.001) on the potentiation of sIPSC frequency but not amplitude ($F_{3,36}$=2.2, P=0.14). Also, we observed a significant interaction between treatment and sex in the potentiation of sIPSC frequency ($F_{3,36}$=19.9, P=0.001) but not amplitude ($F_{3,36}$=3.8, P=0.059). Asterisk denotes statistical significance.

Figure 3. Effect of MRN (VGLUT3) axon terminal activation on GABAergic transmission in IL-mPFC pyramidal neurons.

A) Although 10 Hz light stimulation showed a delayed effect on sIPSC frequency in the IL-mPFC pyramidal neurons from female mice ($F_{1,19}$=4.45, P=0.048, last 15 min), overall frequency ($F_{1,19}$=3.03, P=0.09) and amplitude ($F_{1,19}$=0.92, P=0.34) of sIPSCs following the light activation did not reveal a statistically significant effect between MRN (VGLUT3)-ChR2 group (12

neurons/5 mice) and MRN-EGFP group (9 neurons/5 mice). **B**) The 10 Hz light activation did not affect either frequency ($F_{1,16}$=0.02, P=0.88) or amplitude ($F_{1,16}$=0.07, P=0.78) of sIPSCs in the IL-mPFC pyramidal neurons from male MRN (VGLUT3)-ChR2 group (9 neurons/5 mice) compared to MRN-EGFP group (9 neurons/5 mice). The upper panel shows example traces. Scale: 100 pA/250 ms. A two-way ANOVA did not show a significant effect of sex on sIPSC frequency ($F_{3,38}$=0.2, P=0.6) or amplitude ($F_{3,38}$=0.14, P=0.7). Also, we did not observe a significant interaction between treatment and sex on sIPSC frequency ($F_{3,38}$=2.2, P=0.15) or amplitude ($F_{3,38}$=0.004, P=0.95). Asterisk denotes statistical significance.

Figure 4. Activation of MRN (VGLUT3) axon terminals suppresses excitatory synaptic transmission in the PL-mPFC pyramidal neurons of female mice.

The upper panel shows a schematic of whole-cell recording of EPSPs in layer 5 pyramidal neurons by field stimulation of layer 2/3 and applying 10Hz light stimulation to activate MRN (VGLUT3) terminals. **A**) A 10 Hz light stimulation for 60 s showed suppression of EPSP slope ($F_{1,19}$=5.6, P=0.02) in the PL-mPFC pyramidal neurons from female MRN (VGLUT3)-ChR2 group (12 neurons/6mice) compared to MRN-EGFP group (9 neurons/5 mice). **B**) Light stimulation at 10 Hz did not affect EPSP slope ($F_{1,17}$=0.67, P=0.4) in the PL-mPFC pyramidal neurons from male MRN (VGLUT3)-ChR2 group (10 neurons/5mice) compared to MRN-EGFP group (9 neurons/5 mice). A two-way ANOVA showed a significant effect of sex ($F_{3,38}$=4.47, P=0.04) on the suppression of EPSP slope in the PL-mPFC. We did not observe a significant interaction between treatment and sex on changes in EPSP slope ($F_{3,38}$=0.001, P=0.98). **C**) The IL-mPFC pyramidal neurons from the female MRN (VGLUT3)-ChR2 group (9 neurons/6mice) did not show a change in EPSP slope ($F_{1,16}$=0.4, P=0.85) compared to MRN-EGFP group (9 neurons/5 mice) after the 10 Hz light

stimulation. **D**) Although the IL-mPFC pyramidal neurons from male MRN (VGLUT3)-ChR2 group (10 neurons/5mice) showed a delayed suppression of EPSP slope after the light stimulation (last 5 min, $F_{1,18}$=6.36, P=0.02), a comparison of overall data in MRN (VGLUT3)-ChR2 and MRN-EGFP (10 neurons/5 mice) groups after the light activation did not show a statistically significant effect ($F_{1,18}$=1.5, P=0.23). The inset shows example traces. Scale: 1 mV/25 ms. A two-way ANOVA did not show a significant effect of sex ($F_{3,37}$=1.2, P=0.27) or interaction between treatment and sex on the EPSP slope in the IL-mPFC ($F_{3,37}$=0.7, P=0.4). Asterisk denotes statistical significance.

Figure 5. Activation of MRN (VGLUT3) neurons suppresses fear memory in female mice.

A) A schematic of viral injection into the MRN and an example of a brain slice from VGLUT3 Cre mice showing mCherry-expressing MRN (VGLUT3) neurons 3 weeks after the injection of AAV-hSyn-DIO-hM3D(Gq)-mCherry. **B**) An example trace showing the induction of action potentials in a hM3D(Gq)-expressing MRN (VGLUT3) neuron after the perfusion of CNO (5 µM). Scale: 50 mV/100 s. **C**) Intraperitoneal injection of CNO (1 mg/kg, n=10) but not saline (n=9) 1 hr before extinction training caused a decrease in freezing during the early trials of extinction training (initial 3 trials) in female mice, suggesting suppression of fear memory ($F_{1,17}$=7.8, P=0.01). **D**) Freezing in CNO (n=10)- and saline (n=10)-treated male groups did not show a statistically significant effect ($F_{1,18}$=0.25, P=0.62). A two-way ANOVA did not show a significant effect of sex on freezing during early trials (initial 3 trials) of extinction training ($F_{3,38}$=2.4, P=0.12). However, a significant interaction between treatment and sex was observed ($F_{3,38}$=6.2, P=0.01). **E**) An example trace showing the suppression of action potentials in a spontaneously

firing hM4D(Gi)-expressing MRN (VGLUT3) neuron after the perfusion of CNO (5 μM). Scale: 50 mV/100 s. **F**) CNO (n=14) and saline (n=13) treatment in hM4D(Gi)-expressing female mice did not show a significant difference in freezing ($F_{1,25}$=0.001, P=0.99). **G**) CNO (n=9) and saline (n=9) treatment in hM4D(Gi)-expressing male mice did not show a significant difference in freezing ($F_{1,16}$=0.12, P=0.73). Arrows indicate the injection of saline/CNO. A two-way ANOVA showed an effect of sex on freezing during early trials (initial 3 trials) of extinction training ($F_{3,44}$=8.2, P=0.001). However, we did not observe a significant interaction between treatment and sex ($F_{3,44}$=0.001, P=0.98). Asterisk denotes statistical significance.

Figure 6. Fear conditioning enhances excitatory synaptic transmission in the MRN (VGLUT3) neurons of female mice.

A) A schematic of MRN slice preparation and the recording of tdTomato-expressing MRN (VGLUT3) neurons. **B**) Comparison of mEPSCs and mIPSCs in MRN (VGLUT3) neurons from female TA (13 neurons/6 mice), FC (13 neurons/6 mice), and FE (16 neurons/6 mice) groups. Neurons from the female FC group showed a significantly higher mEPSC amplitude than the TA group. Fear extinction did not affect the increased mEPSC amplitude in the FC group ($F_{2,15}$=8.3, P=0.004, TA vs. FC: P=0.006, TA vs. FE: 0.016, FC vs. FE: P=1). FC and FE treatment did not affect mEPSC frequency ($F_{2,15}$=0.24, P=0.78), mIPSC amplitude ($F_{2,15}$=0.98, P=0.39), or mIPSC frequency ($F_{2,15}$=1.05, P=0.37). The upper panel shows examples of mIPSCs (upper continuous traces) and mEPSCs (lower continuous traces and single events), Scale: 50 pA/500 ms (continuous traces) and 10 pA/10 ms (single events). **C**) Comparison of mEPSCs and mIPSCs in MRN (VGLUT3) neurons from male TA (13 neurons/5 mice), FC (15 neurons/6 mice), and FE (16 neurons/6 mice) groups. The FC and FE treatment did not affect mEPSC amplitude ($F_{2,14}$=0.5, P=0.6), mEPSC frequency ($F_{2,14}$=1.02, P=0.38), mIPSC amplitude ($F_{2,14}$=0.03, P=0.97), or mIPSC

frequency ($F_{2,14}$=0.24, P=0.79). A two-way ANOVA on mEPSC amplitude showed a significant interaction between treatment (TA, FC, and FE) and sex ($F_{5,34}$=3.5, P=0.04) without an effect of sex ($F_{5,34}$=1.8, P=0.18). A two-way ANOVA on mEPSC frequency (effect of sex: $F_{5,34}$=2.9, P=0.09, interaction between treatment and sex: $F_{5,34}$=0.9, P=0.4), mIPSC amplitude (effect of sex: $F_{5,34}$=1.7, P=0.2, interaction between treatment and sex: $F_{5,34}$=0.09, P=0.9), mIPSC frequency (effect of sex: $F_{5,34}$=0.73, P=0.38, interaction between treatment and sex: $F_{5,34}$=0.9, P=0.4) did not show sex-specific effects. Comparison of mEPSC amplitude, mEPSC frequency, mIPSC amplitude, and mIPSC frequency in TA groups revealed sex difference in mEPSC amplitude (P=0.02). Asterisk denotes statistical significance.

Figure 7. PL-mPFC (VGLUT3) neuron-mediated synaptic transmission shows sex difference.

A) A schematic of light activation of PL-mPFC (VGLUT3) neurons and whole-cell recording in local SST and pyramidal neurons. **B**) EPSC amplitude, IPSC amplitude, and excitatory/inhibitory ratio (E/I ratio) in PL-mPFC (SST) neurons in response to light activation of PL-mPFC (VGLUT3) neurons. These measurements were made before the application of any drugs. Both the EPSC amplitude (P=0.04) and IPSC amplitude (P=0.01) were significantly higher in female mice [29 neurons (16 female mice) and 23 neurons (13 male mice)]. The E/I ratio did not show a significant sex difference (P=0.56). The left panel shows an example of monosynaptic EPSC and IPSC in an SST neuron. 4-AP rescues TTX-induced suppression of EPSC and IPSC, the monosynaptic nature of which is revealed in the presence of AMPA and NMDA receptor blockers (DNQX+AP5). The addition of bicuculline confirmed the GABAergic nature of IPSCs. Scale 50pA/5ms. **C**) EPSC amplitude, IPSC amplitude, and E/I ratio in PL-mPFC (pyramidal) neurons in response to light activation of PL-mPFC (VGLUT3) neurons. Neither EPSC amplitude (P=0.28) nor IPSC

amplitude (P=0.36) showed a significant sex difference [12 neurons (5 female mice) and 13 neurons (5 male mice)]. However, the E/I ratio showed a significant sex difference (P=0.04). The left panel shows an example of monosynaptic EPSC and IPSC in a pyramidal neuron. 4-AP rescues TTX-induced suppression of EPSC and IPSC, the monosynaptic nature of which is revealed in the presence of AMPA and NMDA receptor blockers (DNQX+AP5). The addition of bicuculline confirmed the GABAergic nature of IPSCs. Scale 50pA/5ms. Blue line indicates light application. Asterisk denotes statistical significance.

Materials and Methods

Animals

Both female and male mice (3-6 months old) were used in experiments. B6;129S-*Slc17a8*$^{tm1.1(cre)Hze}$/J (Stock number: 028534, Jackson Laboratories) mice were used for studying the effect of optogenetic and chemogenetic activation. B6;129S-*Slc17a8*$^{tm1.1(cre)Hze}$/J mice were crossed with C57BL/6J (Stock number: 000664, Jackson Laboratories) for breeding. We crossed B6;129S-*Slc17a8*$^{tm1.1(cre)Hze}$/J mice with GIN mice (FVB-Tg(GadGFP)45704Swn/J, Stock number: 003718, Jackson Laboratories) and G42 mice (CB6-Tg(Gad1-EGFP)G42Zjh/J, Stock number: 007677, Jackson Laboratories) to generate mice that are positive for Cre in VGLUT3 neurons and EGFP in SST and PV neurons, respectively [27,41]. VGLUT3-tdTomato mice were created by crossing B6;129S-*Slc17a8*$^{tm1.1(cre)Hze}$/J with B6.Cg-*Gt(ROSA)26Sor*$^{tm14(CAG-tdTomato)Hze}$/J (Stock number: 007914, Jackson Laboratories) [42]. Mice were maintained on a 12-hour light-dark cycle at 23ºC with access to food and water ad libitum. The Institutional Animal Care and Use Committee of the University of Toledo approved all the procedures.

Stereotactic surgery

Viral injections were performed on a stereotactic apparatus (Stoelting, IL, USA) under isoflurane anesthesia. 200 nl AAV-EF1a-double floxed-hChR2(H134R)-mCherry-WPRE-HGHpA (AAV9), AAV-EF1a-double floxed-hChR2(H134R)-EYFP-WPRE-HGHpA (AAV9), AAV-hSyn-EGFP (AAV2), AAV-hSyn-DIO-hM3D(Gq)-mCherry (AAV2), AAV-hSyn-DIO-hM4D(Gi)-mCherry (AAV2) and AAV-hSyn-DIO-EGFP (AAV2) were injected at a rate of 100 nl/min using an injector (Nanoliter 2010, WPI, FL, USA) attached to a pulled glass injection micropipette (~50 µm tip, Item no: 504949, WPI, FL, USA). Injection coordinates for MRN were (from bregma): AP: -3.6mm; ML: 1.2mm, DV: 4.6mm, 16° angle (ear bars at 18mm, anesthesia

mask bar at 14mm). Injection coordinates for mPFC were (from bregma): AP: 2.1mm; ML: 0.8mm, DV: 2.6mm, 16° angle (ear bars at 18mm, anesthesia mask bar at 14mm). The accuracy of virus injections was confirmed using fluorescence microscopy to visualize mCherry/EGFP/EYFP-expressing neurons. Injected mice were used for electrophysiology and behavior experiments 3 weeks after the surgery.

Electrophysiology

Following transcardial perfusion with ice-cold oxygenated artificial cerebrospinal fluid (ACSF) containing (in mM): NaCl (118), glucose (10), KCl (2.5), NaH_2PO_4 (1), $CaCl_2$ (1) and $MgSO_4$ (1.5) (325 mOsm, pH 7.4) under pentobarbital (120mg//kg) anesthesia, brains were isolated for preparing prefrontal cortical (300 µm) and MRN (200 µm) slices on a vibratome (Campden Instruments). Prefrontal cortical slices were incubated in ACSF at room temperature for a minimum of 1 hr, followed by the transfer of brain slices to the recording chamber superfused with the ACSF containing 2.5 mM $CaCl_2$ at 32°C flowing at 2 ml/min rate. MRN slices were transferred to oxygenated ACSF at 35°C and allowed to recover for at least 1 hr, during which the ACSF cooled down to room temperature. Both the mPFC and MRN were located using a 4X objective. Recorded neurons were visualized using a 40X water immersion objective and video-enhanced differential interference contrast microscopy. EGFP- and tdTomato-expressing neurons were identified using fluorescence microscopy, while pyramidal neurons were identified by their morphology, location, and membrane characteristics. MRN (VLGUT3) neuron-mediated currents, the effect of 10Hz stimulation on EPSPs, and membrane properties in mPFC and MRN (VGLUT3) neurons were recorded using recording electrodes of 3–5 MΩ resistance filled with an internal solution containing (in mM): K-gluconate (130), KCl (10), $MgCl_2$ (5), MgATP (5), NaGTP (0.2), HEPES (5), pH adjusted to 7.4 with KOH. EPSPs were evoked at 0.1 Hz in layer 5 pyramidal

neurons by electrical stimulation (100-200 μA) of layer 2/3 using an extracellular stimulating electrode (FHC, ME, USA). Membrane properties in mPFC pyramidal neurons were recorded before and 25 min after the 10Hz light stimulation. The effect of 10Hz light stimulation on sIPSCs in pyramidal neurons was recorded using an internal solution containing (in mM): K-gluconate (130), KCl (5), $MgCl_2$ (2), MgATP (5), NaGTP (0.2), HEPES (5), pH adjusted to 7.4 with KOH. sIPSCs were recorded in pyramidal neurons at 0 mV. These $GABA_A$ receptor-mediated sIPSCs were confirmed using bicuculline (10 μM). mEPSCs and mIPSCs were recorded from MRN (VGLUT3) neurons at -50 mV and 0 mV, respectively, in the presence of tetrodotoxin (1 μM). AMPA receptor-mediated mEPSCs, and $GABA_A$ receptor-mediated mIPSCs were confirmed using DNQX (10 μM) and bicuculline (10 μM), respectively. An internal solution containing (in mM): Cesium methanesulfonate (130), NaCl (6), HEPES (5), MgATP (5), NaGTP (0.2), pH adjusted to 7.4 with CsOH was used for recording mEPSCs and mIPSCs in MRN (VGLUT3) neurons. mPFC (VGLUT3) neuron-mediated transmission in SST, PV, and pyramidal neurons was recorded at -20mV using an internal solution containing (in mM): K-gluconate (130), KCl (2), $MgCl_2$ (2), MgATP (5), NaGTP (0.2), HEPES (5), pH adjusted to 7.4 with KOH. Blue light (470 nm) was emitted from a Lumen 1600-LED (Prior) for optogenetic experiments. The PL-mPFC (VGLUT3) neuron-mediated EPSC and IPSC amplitudes were calculated before drug application. Electrophysiological recordings were rejected when series resistance or holding current changed by 10% or more.

Behavior

A mouse was placed in the conditioning chamber (context A) within a soundproof box (Actimetrics, IL, USA) for fear conditioning. After a 2 min exploration, mice received 2 habituation tones (5 kHz, 30Db, 30 s duration) followed by 3 tones (30 s duration) that co-

terminated with foot shocks (2 s duration, 0.5 mA, 30 s interval). Mice were returned to their home cages 30 s after the final tone-shock pairing. The control tone-alone (TA) group received tone presentations similar to the fear-conditioned (FC) group, except they did not receive foot shocks. Fear-extinction (FE) training was carried out 24 hr after conditioning and consisted of 30 tone presentations (30 s duration) at 30 s intervals (context B). For all groups, fear memory was tested 48 hr after the initial fear conditioning/tone alone treatment by exposing the mice to 3 tones (30 s duration) at 30 s intervals (context B). Freezing was measured using FreezeFrame software (Actimetrics, IL, USA). For studying the effect of chemogenetic activation or suppression of MRN (VGLUT3) neurons on fear memory, fear-conditioned mice received either saline or CNO (1 mg/kg, intraperitoneal) 1 hr before fear extinction training. In control experiments to confirm the lack of a non-specific effect of CNO on fear memory and extinction, CNO or saline was administered to mice that received the AAV-hSyn-EGFP injection into the MRN. For the experience-dependent plasticity experiments, brain slices were prepared within 4 hr after the fear memory test.

Immunohistochemistry and microscopy

Under pentobarbital (120mg/kg) anesthesia, mice were transcardially perfused with 4% PFA in PBS. Brains were collected in 4% PFA and stored at 4ºC overnight before being placed in 15% sucrose for 24 hr followed by 30% sucrose for 24 hr at 4ºC. Brains were frozen on dry ice and 45 µm cryosections of the brain slices were placed in PBS before immunohistochemistry experiments. For the immunohistochemistry experiments, brain slices were washed in TBS 3 times for 5 min. Washed slices were blocked with 3% normal goat serum and 0.3% Triton X in TBS for 30 minutes at room temperature. The slices were then incubated in mCherry polyclonal antibody (Rockland Immunochemicals, Cat. No. 600401P16) at a dilution of 1:1000 in 0.3% Triton-X/TBS

for 24 hr at 4 °C [43]. Slices were rinsed 3 times in TBS for 5 min and transferred to goat anti-rabbit IgG (H+L) Alexa Fluor™ 594 (Invitrogen, Cat. No. A11037, RRID: AB_2534095) with a dilution of 1:1000 in 0.3% Triton-X/TBS and 5% Normal Goat Serum for 2 hr incubation at room temperature. Slices were then rinsed 3 times in TBS for 5 min, mounted on Superfrost Plus microscope slides, and coversliped with Fluoromount-G with DAPI (Southern Biotech, Cat# 0100–20).

Confocal images of the PL-mPFC were taken from 3 sections for each animal, using a TCS SP5 multiphoton laser-scanning confocal microscope (Leica Microsystems, Buffalo Grove, IL) with a 20X objective lens. Maintaining the same laser intensity, exposure time, camera gain, and neutral density filter settings, Z-stack images (1-µm optical sections) were acquired, and 3D projections were constructed with the Leica AFM acquisition/analytical software suite. Images taken for fiber density analysis were taken as large Z-stack tiles and then cropped to 400 x 600 µm using Lecia Application Suite X to cover only the area of interest. By using a methodology described earlier [44,45], confocal images were converted to grayscale 8-bit images and feature-extracted for mCherry-expressing VGLUT3 fibers through a Hessian-based filter in NIH ImageJ (version 1.44) software plugin, FeatureJ. FeatureJ-based filtering of images was performed utilizing the smallest eigenvalue of Hessian tensor option (smoothing scale 1). The image was then converted to a binary image using an auto threshold value determined to depict fibers in test images accurately. A blind observer analyzed the images, and the average intensity was determined using the analyze function in ImageJ.

Data analysis

We used Clampfit 10.7 (Molecular Devices, CA, USA) for analyzing synaptic responses and membrane properties. EPSP slope was measured at the initial 2 ms of EPSP response.

Membrane properties were analyzed as described before, and frequency and accommodating properties of action potentials and shape, capacitance, and location of neurons were used in identifying pyramidal neurons [31,45,46]. Statistical analyses were performed using IBM SPSS statistics (version 27) or GraphPad Prism (version 9) software. A two-way ANOVA followed by the Bonferroni post hoc test or t-test was used for analyzing spontaneous currents, EPSPs, membrane properties, and behavioral data. Data from experience-dependent plasticity experiments were averaged per mouse before the statistical analysis. The effect of sex on sIPSCs and EPSPs was analyzed at 15 min after the 10Hz stimulation.

Figure 1

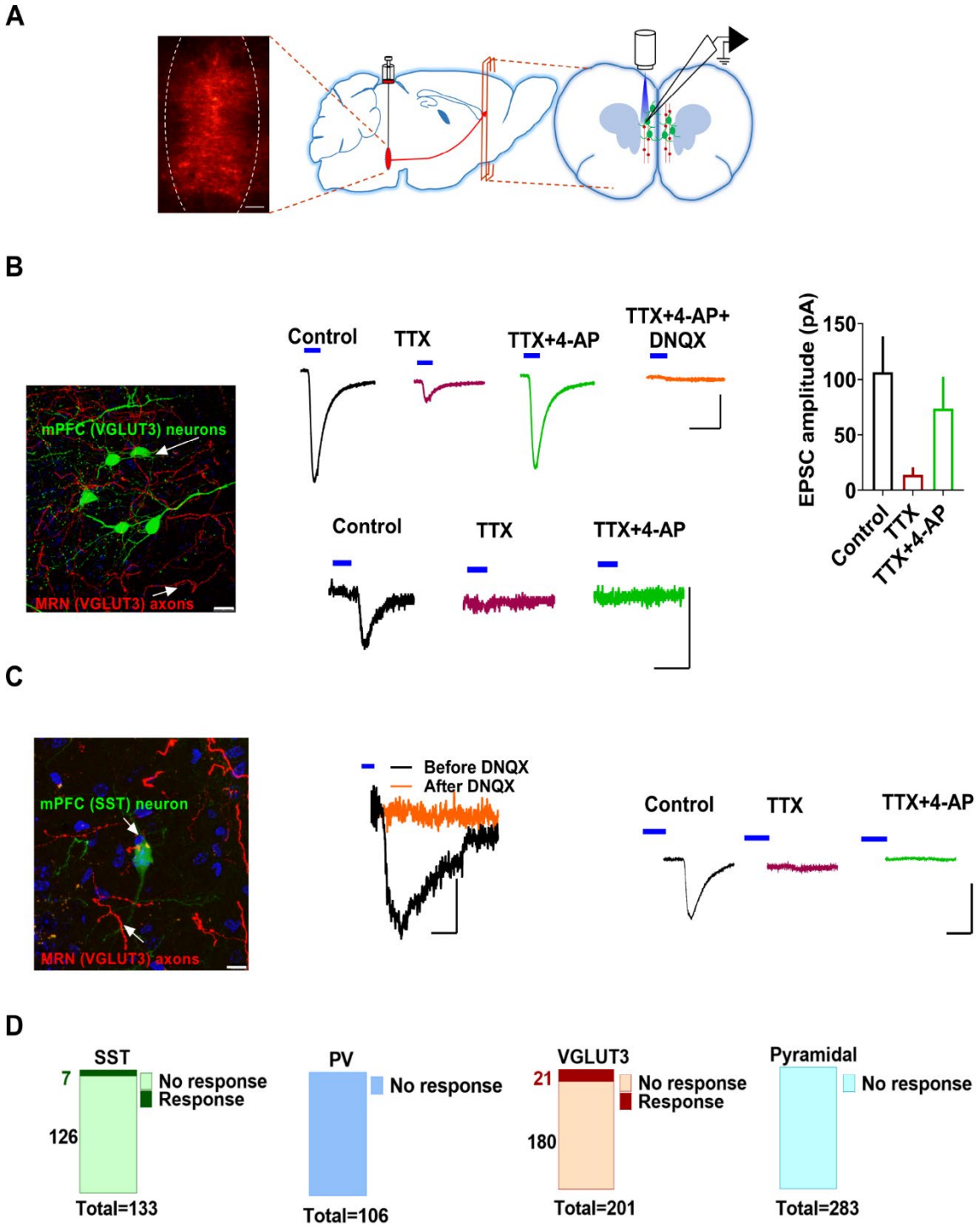
A
B
mPFC (VGLUT3) neurons
MRN (VGLUT3) axons
Control
TTX
TTX+4-AP
TTX+4-AP+
DNQX
Control
TTX
TTX+4-AP
EPSC amplitude (pA)
150
100
50
0
Control
TTX
TTX+4-AP
C
mPFC (SST) neuron
MRN (VGLUT3) axons
Before DNQX
After DNQX
Control
TTX
TTX+4-AP
D
SST
7
126
No response
Response
Total=133
PV
No response
Total=106
VGLUT3
21
180
No response
Response
Total=201
Pyramidal
No response
Total=283

Figure 2

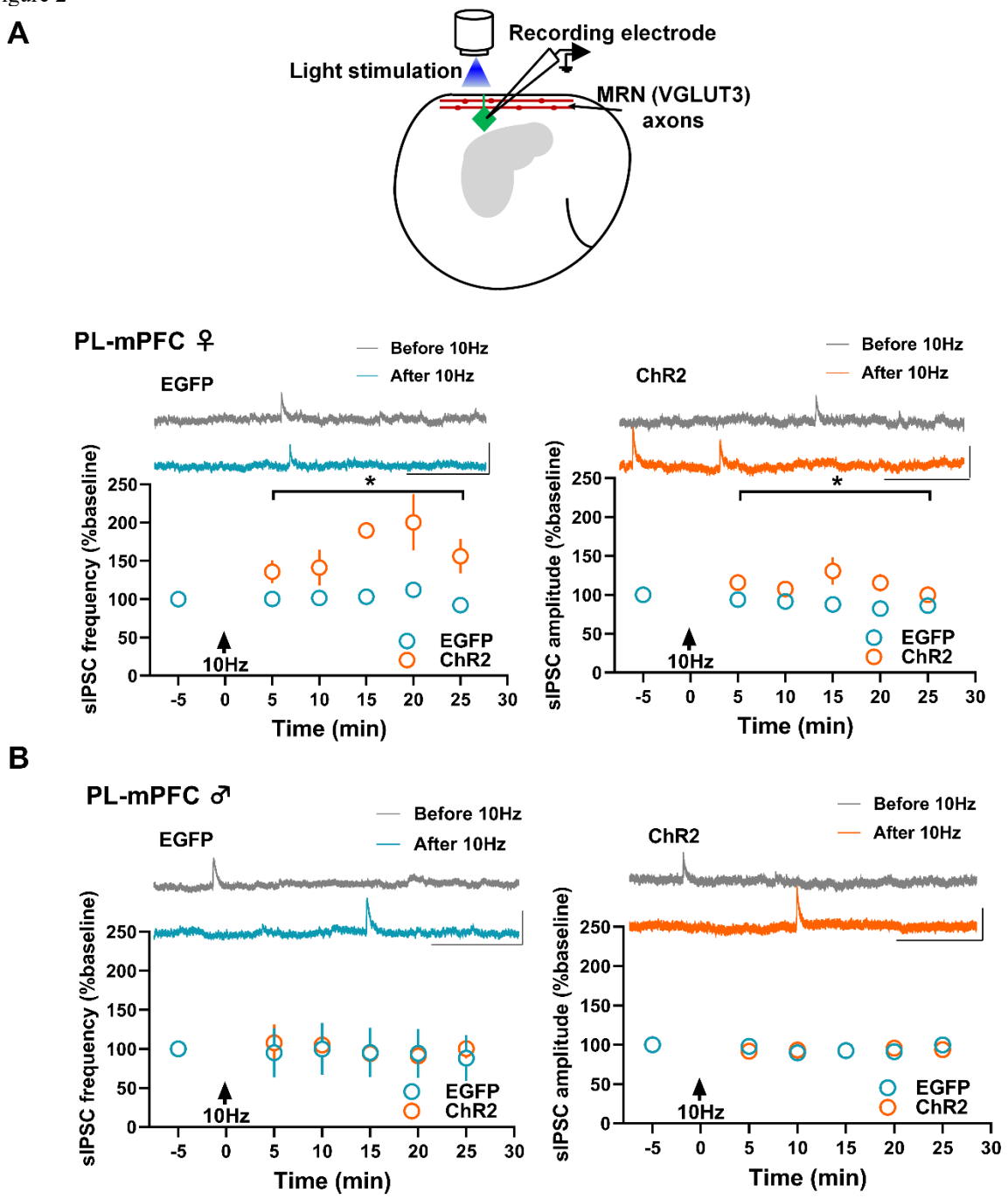
A
Recording electrode
Light stimulation
MRN (VGLUT3)
axons
PL-mPFC ♀
EGFP
Before 10Hz
After 10Hz
sIPSC frequency (%baseline)
10Hz
EGFP
ChR2
Time (min)
ChR2
sIPSC amplitude (%baseline)
B
PL-mPFC ♂

Figure 3

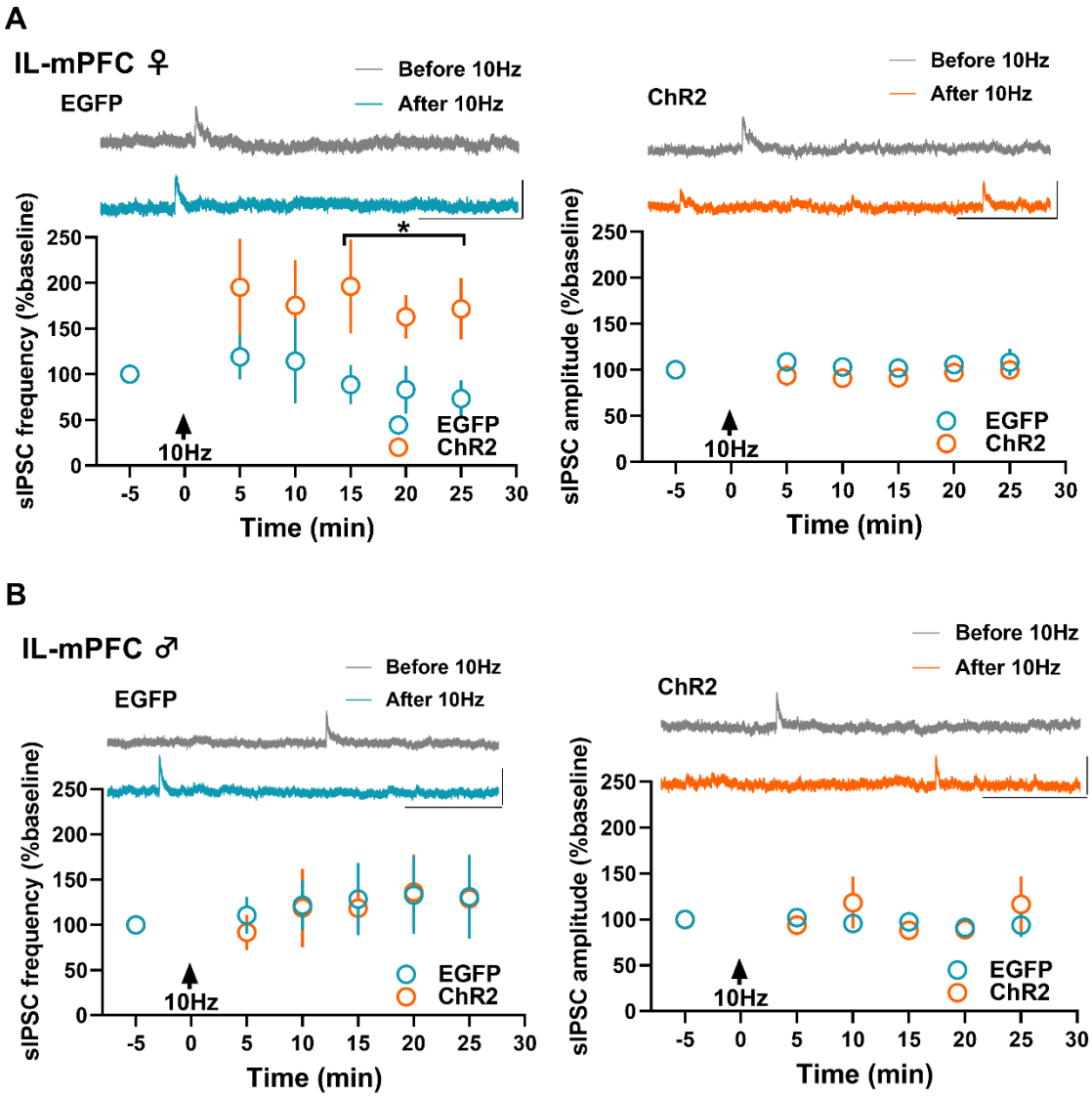
A
IL-mPFC ♀
EGFP
Before 10Hz
After 10Hz
sIPSC frequency (%baseline)
250
200
150
100
50
0
*
10Hz
EGFP
ChR2
-5
0
5
10
15
20
25
30
Time (min)
ChR2
Before 10Hz
After 10Hz
sIPSC amplitude (%baseline)
250
200
150
100
50
0
10Hz
EGFP
ChR2
-5
0
5
10
15
20
25
30
Time (min)
B
IL-mPFC ♂
EGFP
Before 10Hz
After 10Hz
sIPSC frequency (%baseline)
250
200
150
100
50
0
10Hz
EGFP
ChR2
-5
0
5
10
15
20
25
30
Time (min)
ChR2
Before 10Hz
After 10Hz
sIPSC amplitude (%baseline)
250
200
150
100
50
0
10Hz
EGFP
ChR2
-5
0
5
10
15
20
25
30
Time (min)

Figure 4

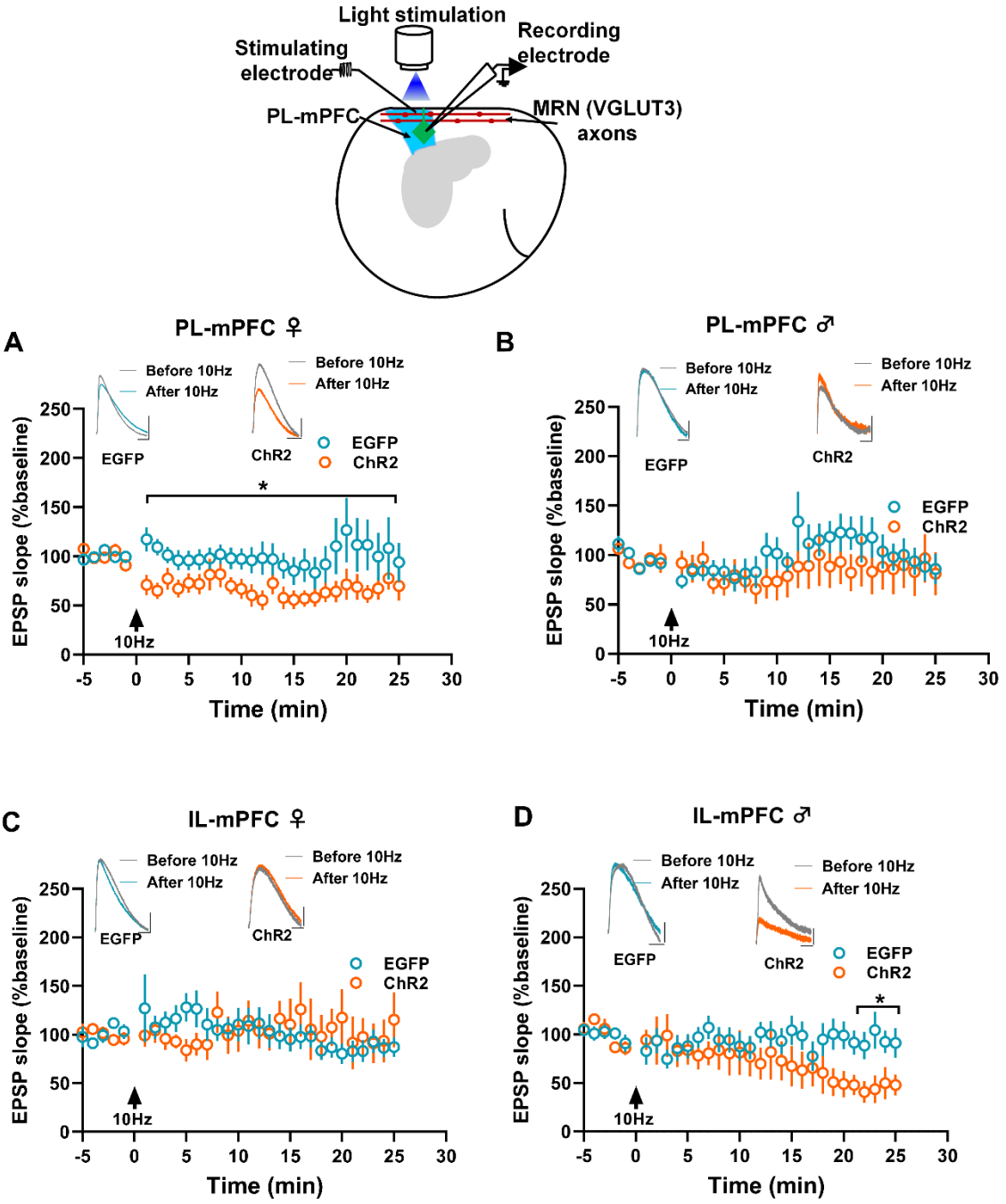
Light stimulation
Stimulating electrode
Recording electrode
PL-mPFC
MRN (VGLUT3) axons
A
PL-mPFC ♀
B
PL-mPFC ♂
C
IL-mPFC ♀
D
IL-mPFC ♂
Before 10Hz
After 10Hz
EGFP
ChR2
EPSP slope (%baseline)
Time (min)
10Hz
*

Figure 5

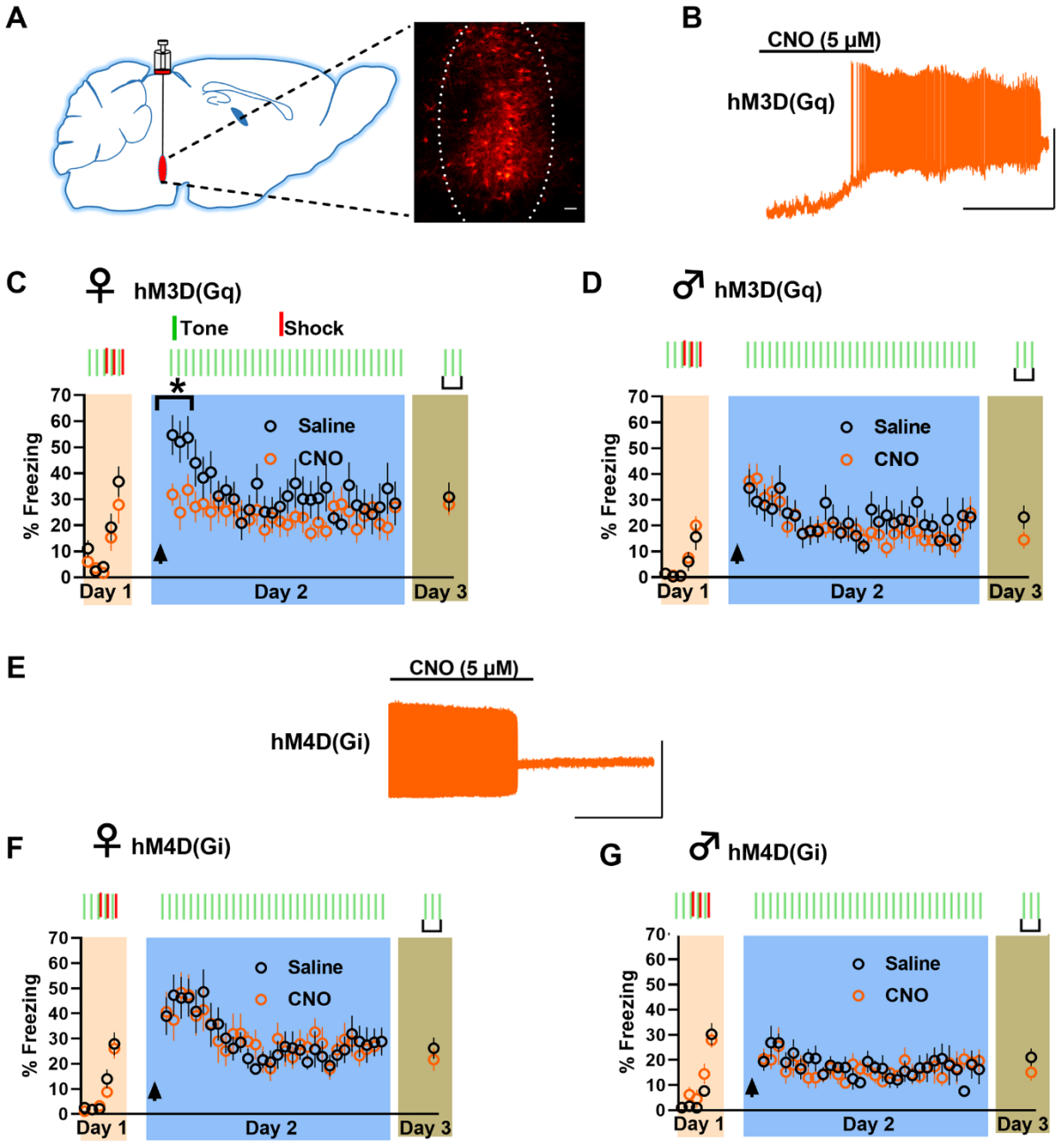
A
B
CNO (5 μM)
hM3D(Gq)
C
♀ hM3D(Gq)
Tone
Shock
*
Saline
CNO
% Freezing
Day 1
Day 2
Day 3
D
♂ hM3D(Gq)
E
CNO (5 μM)
hM4D(Gi)
F
♀ hM4D(Gi)
G
♂ hM4D(Gi)

Figure 6

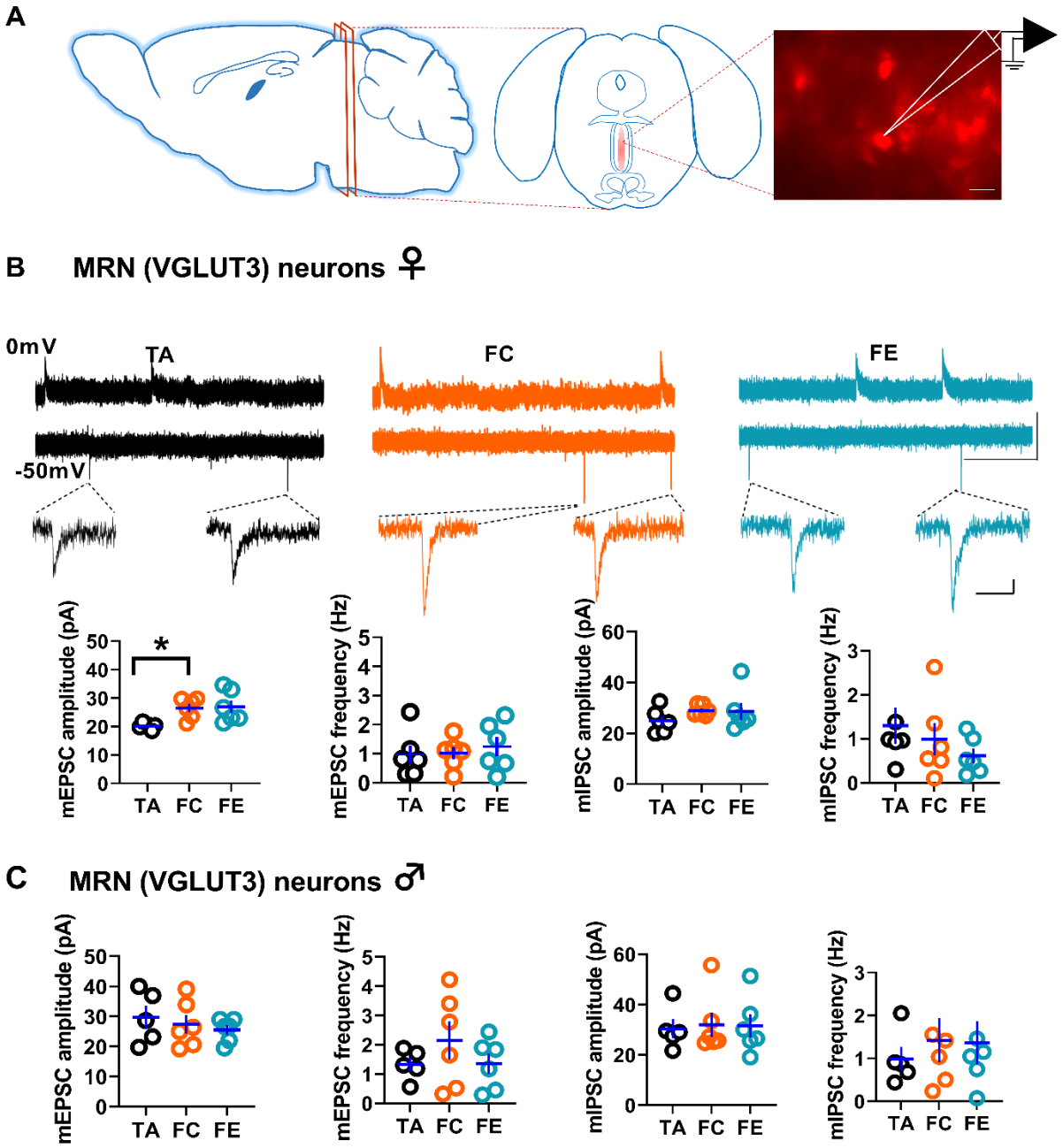
A
B MRN (VGLUT3) neurons ♀
0mV
-50mV
TA
FC
FE
mEPSC amplitude (pA)
mEPSC frequency (Hz)
mIPSC amplitude (pA)
mIPSC frequency (Hz)
*
TA FC FE
C MRN (VGLUT3) neurons ♂

Figure 7

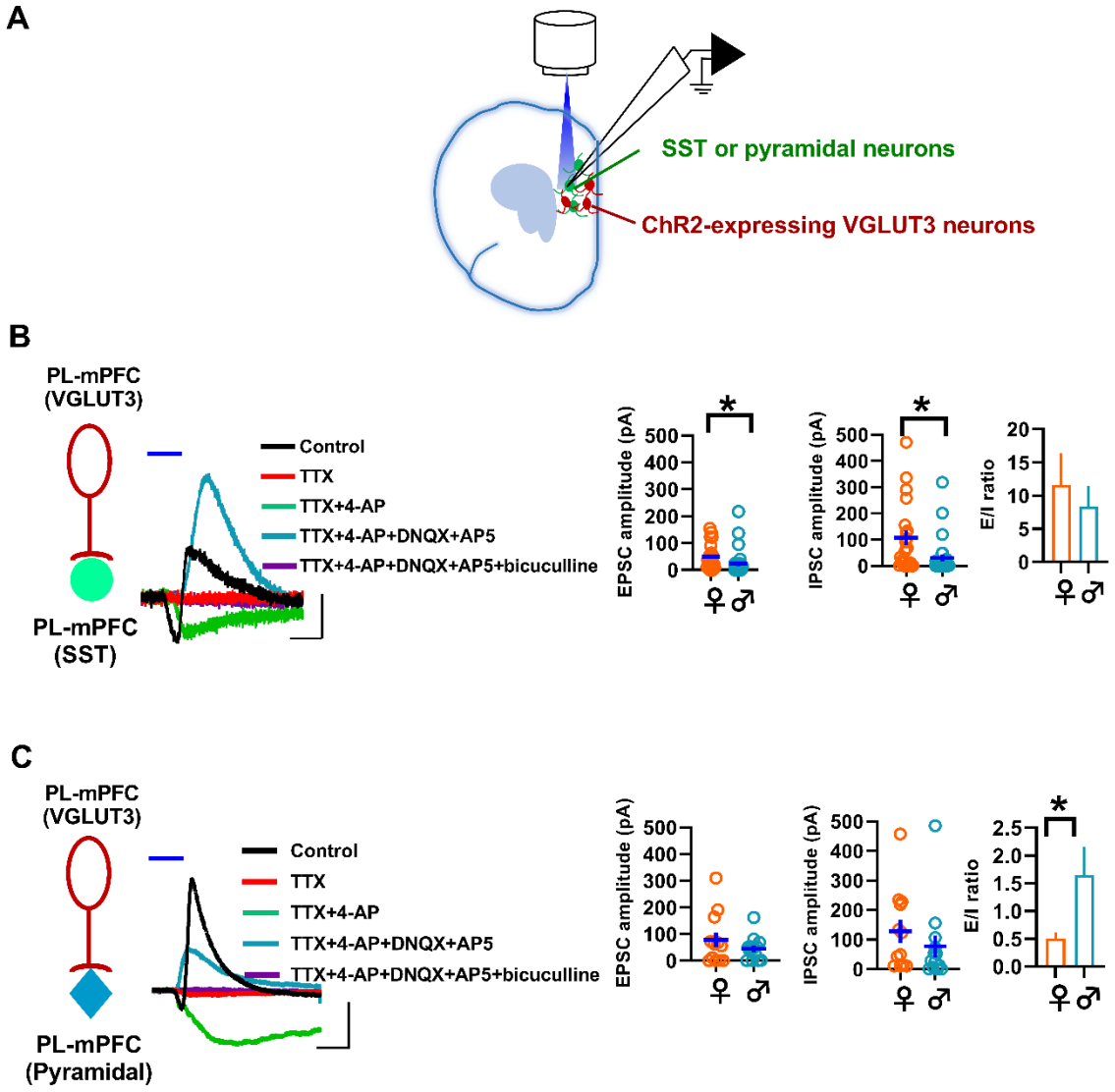
A
SST or pyramidal neurons
ChR2-expressing VGLUT3 neurons
B
PL-mPFC
(VGLUT3)
PL-mPFC
(SST)
Control
TTX
TTX+4-AP
TTX+4-AP+DNQX+AP5
TTX+4-AP+DNQX+AP5+bicuculline
EPSC amplitude (pA)
IPSC amplitude (pA)
E/I ratio
C
PL-mPFC
(VGLUT3)
PL-mPFC
(Pyramidal)
Control
TTX
TTX+4-AP
TTX+4-AP+DNQX+AP5
TTX+4-AP+DNQX+AP5+bicuculline
EPSC amplitude (pA)
IPSC amplitude (pA)
E/I ratio

Legends for supplemental figures

Figure S1 Effect of 10Hz light activation on active and passive membrane properties of PL-mPFC pyramidal neurons from female MRN (VGLUT3)-ChR2 (13 neurons/7 mice) and MRN-EGFP (10 neurons/5 mice) mice, related to Figures 2,4. Light activation did not affect the number of action potentials ($F_{3,42}$=0.45, P=0.72), input resistance (Rin, $F_{3,42}$=0.72, P=0.55), time constant (tau, $F_{3,42}$=1.3, P=0.29), membrane capacitance (Cm, $F_{3,42}$=2.58, P=0.07), or resting membrane potential (RMP, $F_{3,42}$=2.07, P=0.12) in pyramidal neurons. The upper panel shows example traces before and after the 10Hz stimulation in PL-mPFC slices from MRN (VGLUT3)-ChR2 and MRN-EGFP mice. Scale: 50 mV/500 ms.

Figure S2 Effect of 10Hz light activation on active and passive membrane properties of PL-mPFC pyramidal neurons from male MRN (VGLUT3)-ChR2 (12 neurons/6 mice) and MRN-EGFP (12 neurons/6 mice) mice, related to Figures 2,4. Light activation did not affect the number of action potentials ($F_{3,44}$=0.13, P=0.94), input resistance (Rin, $F_{3,44}$=1.8, P=0.16), time constant (tau, $F_{3,44}$=2.49, P=0.07), membrane capacitance (Cm, $F_{3,44}$=0.82, P=0.48), and resting membrane potential (RMP, $F_{3,44}$=2.4, P=0.08) in pyramidal neurons.

Figure S3 Effect of 10Hz light activation on active and passive membrane properties of IL-mPFC pyramidal neurons from female MRN (VGLUT3)-ChR2 (11 neurons/6 mice) and MRN-EGFP (11 neurons/5 mice) mice, related to Figures 3,4. Light activation did not affect the number of action potentials ($F_{3,40}$=0.42, P=0.74), input resistance (Rin, $F_{3,40}$=0.66, P=0.58), time constant (tau, $F_{3,40}$=0.69, P=0.56), membrane capacitance (Cm, $F_{3,40}$=0.71, P=0.55), or resting membrane potential (RMP, $F_{3,40}$=1.4, P=0.26) in pyramidal neurons.

Figure S4 Effect of 10Hz light activation on active and passive membrane properties of IL-mPFC pyramidal neurons from male MRN (VGLUT3)-ChR2 (13 neurons/6 mice) and MRN-EGFP (11

neurons/5 mice) mice, related to Figures 3,4. Light activation did not affect the number of action potentials ($F_{3,44}$=0.16, P=0.92), input resistance (Rin, ($F_{3,44}$=0.52, P=0.67), time constant (tau, $F_{3,44}$=1.01, P=0.4), membrane capacitance (Cm, $F_{3,44}$=0.59, P=0.63), and resting membrane potential (RMP, $F_{3,44}$=1.4, P=0.25) in pyramidal neurons.

Figure S5 MRN (VGLUT3) fiber density in the PL-mPFC from female and male MRN (VGLUT3)-ChR2 mice, related to Figures 2-4. Comparison of the density of mCherry-expressing axons in the PL-mPFC from 3 female and 3 male MRN (VGLUT3)-ChR2 mice did show a statistically significant difference (P=0.59). The left panel shows example images. Scale 50 μm.

Figure S6 Control experiments for fear behavior experiments, related to Figure 5. CNO (1 mg/kg)- and saline-treatment in female (**A**) [(CNO, n=10, saline, n=10), ($F_{1,18}$=0.17, P=0.68)] and male (**B**) [(CNO, n=9, saline, n=9), ($F_{1,16}$=0.2, P=0.8)] C57BL6/J mice that received a pAAV-hSyn-EGFP injection into the MRN did not show a significant difference in fear memory or extinction.

Figure S7 Effect of fear conditioning and extinction on the excitability of MRN (VGLUT3) neurons, related to Figure 6. **A**) Passive and active membrane properties in tdTomato-expressing MRN (VGLUT3) neurons from female tone-alone (TA, 20 neurons/7 mice), fear-condition (FC, 16 neurons/7 mice), and fear-extinction (FE, 15 neurons/6 mice) groups. We did not observe a significant change in the number of action potentials ($F_{2,17}$=2.7, P=0.09), input resistance (Rin, $F_{2,17}$=2.23, P=0.14), time constant (tau, $F_{2,17}$=0.15, P=0.85), membrane capacitance (Cm, $F_{2,17}$=0.38, P=0.69), and resting membrane potential (RMP, $F_{2,17}$=0.8, P=0.46) among TA, FC, and FE groups. The upper panel shows example traces. Scale: 50 mV/500 ms. **B**) We did not observe a significant change in the number of action potentials ($F_{2,15}$=0.2, P=0.82), input resistance (Rin, $F_{2,15}$=0.49, P=0.62), time constant (tau, $F_{2,15}$=0.14, P=0.87), membrane capacitance (Cm, $F_{2,15}$=2.3, P=0.13), and resting membrane potential (RMP, $F_{2,15}$=1.2, P=0.33) among male TA (17 neurons/6

mice), FC (16 neurons/6 mice) and FE (15 neurons/6 mice) groups. A comparison of membrane properties in control TA groups did not show a difference in the number of action potentials ($F_{1,11}$=1.1, P=0.3), input resistance (P=0.25), time constant (P=0.49) or capacitance (P=0.52) between female and male groups. However, the RMP comparison showed a significant depolarization in the female TA group compared to the male TA group (P=0.02).

Figure S8 PL-mPFC (VGLUT3) neuron-mediated glutamatergic and GABAergic currents in local PV neurons, related to Figure 7. **A**) A schematic of light activation of PL-mPFC (VGLUT3) neurons and whole-cell recording in local PV neurons. **B**) EPSC amplitude, IPSC amplitude, and E/I ratio in PL-mPFC (PV) neurons in response to light activation of PL-mPFC (VGLUT3) neurons. We did not observe sex difference in EPSC amplitude (P=0.57), IPSC amplitude (P=0.52), or E/I ratio (P=0.79) [12 neurons (3 female mice) and 9 neurons (3 male mice)]. The left panel shows an example of glutamatergic and GABAergic currents in PV neurons in response to light activation of mPFC (VGLUT3) neurons. Scale 50pA/5ms. Blue line indicates light application.

Figure S1

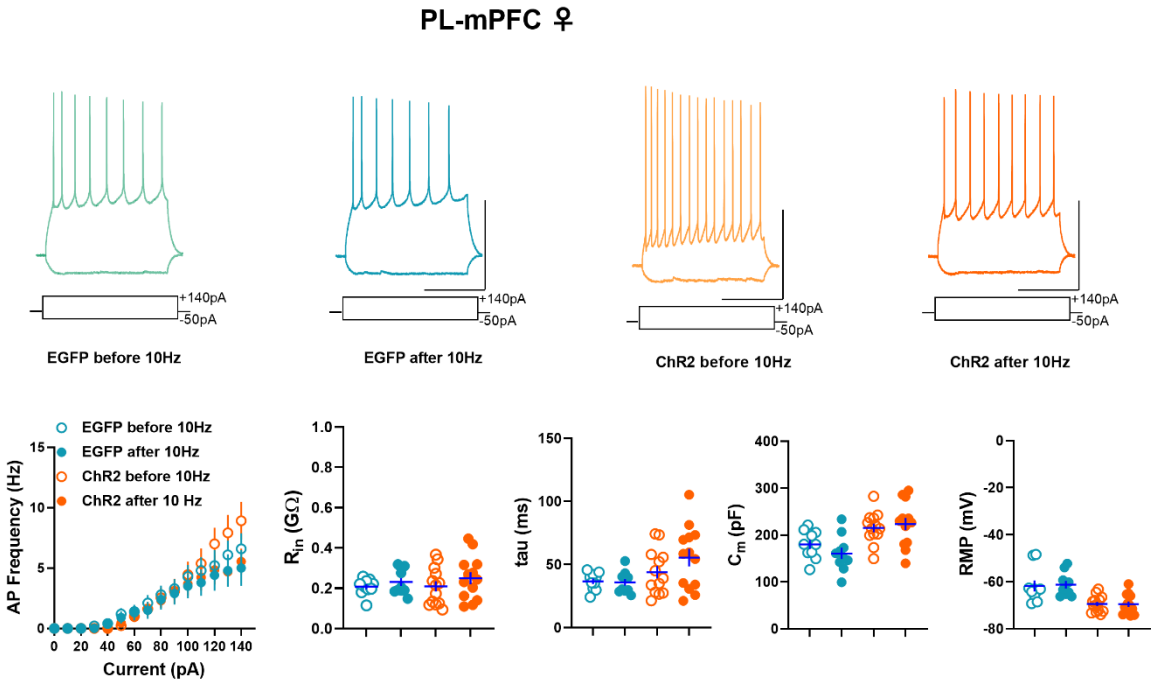
PL-mPFC ♀
+140pA
-50pA
EGFP before 10Hz
EGFP after 10Hz
ChR2 before 10Hz
ChR2 after 10Hz
EGFP before 10Hz
EGFP after 10Hz
ChR2 before 10Hz
ChR2 after 10 Hz
AP Frequency (Hz)
Current (pA)
R_{in} (GΩ)
tau (ms)
C_m (pF)
RMP (mV)

Figure S2

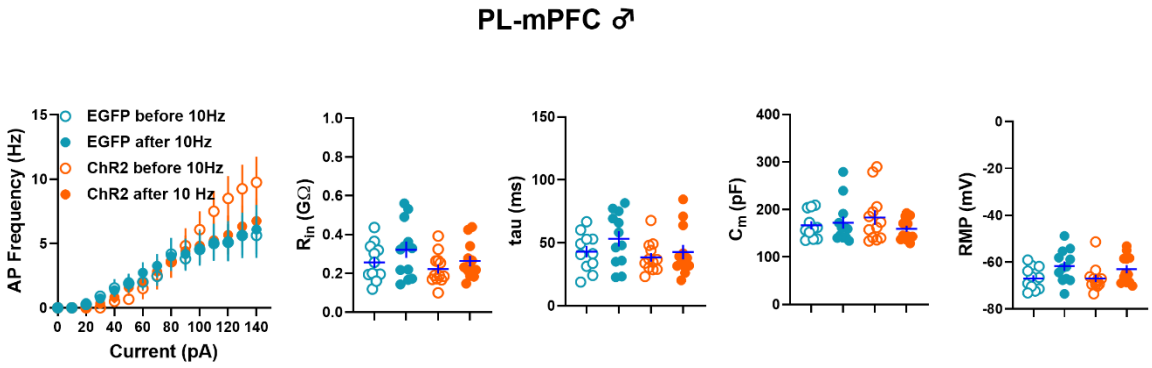
PL-mPFC ♂
EGFP before 10Hz
EGFP after 10Hz
ChR2 before 10Hz
ChR2 after 10 Hz
AP Frequency (Hz)
Current (pA)
R_{in} (GΩ)
tau (ms)
C_m (pF)
RMP (mV)

Figure S3

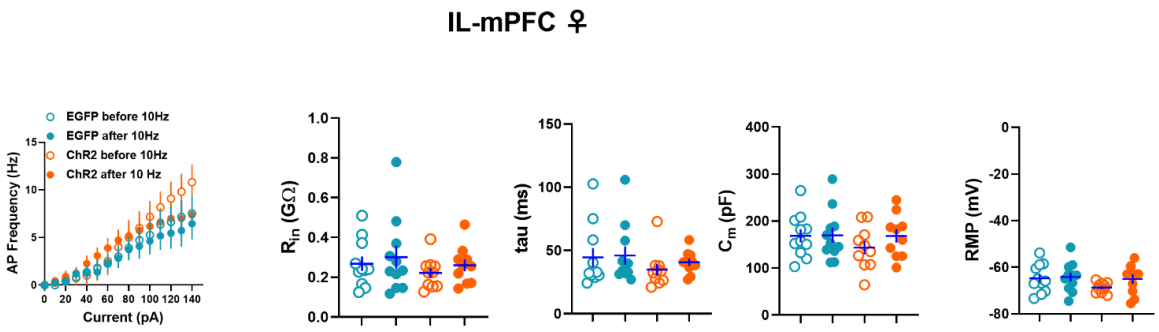
IL-mPFC ♀
EGFP before 10Hz
EGFP after 10Hz
ChR2 before 10Hz
ChR2 after 10 Hz
AP Frequency (Hz)
Current (pA)
R_{in} (GΩ)
tau (ms)
C_m (pF)
RMP (mV)

Figure S4

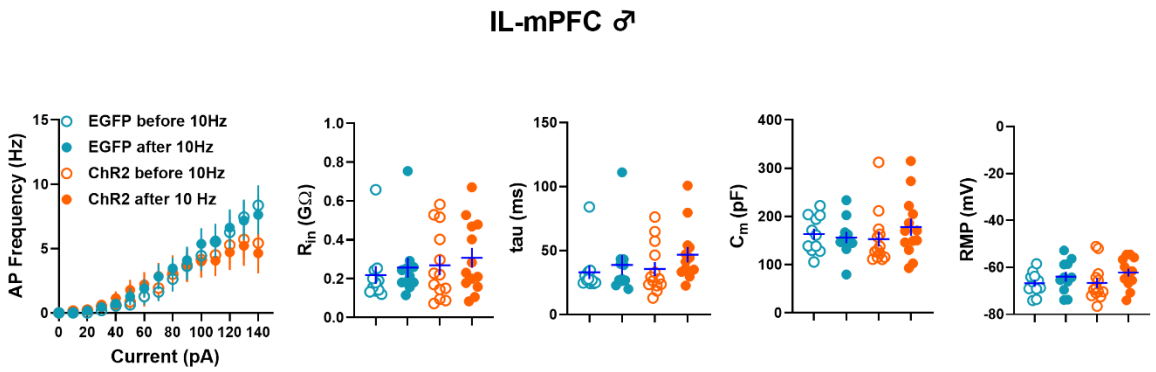
IL-mPFC ♂
EGFP before 10Hz
EGFP after 10Hz
ChR2 before 10Hz
ChR2 after 10 Hz
AP Frequency (Hz)
Current (pA)
R_{in} (GΩ)
tau (ms)
C_m (pF)
RMP (mV)

Figure S5

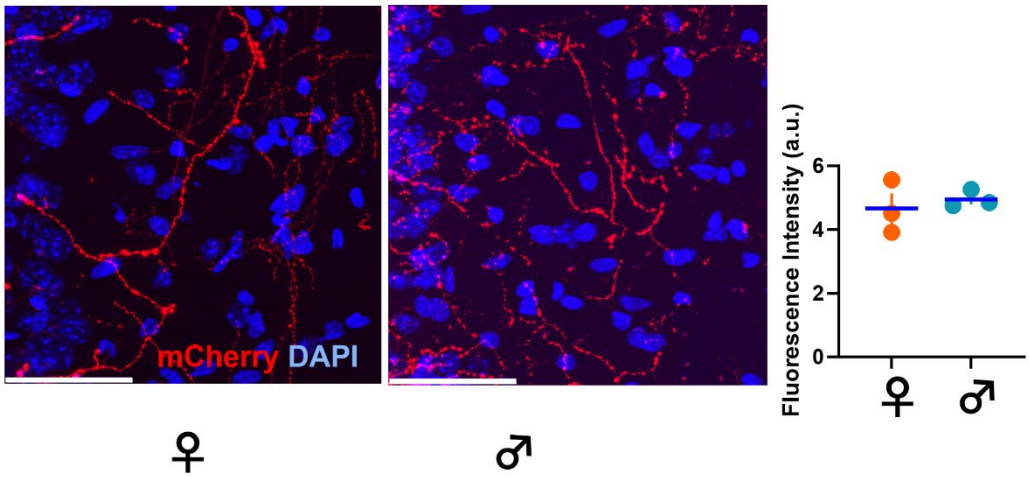

Figure S6

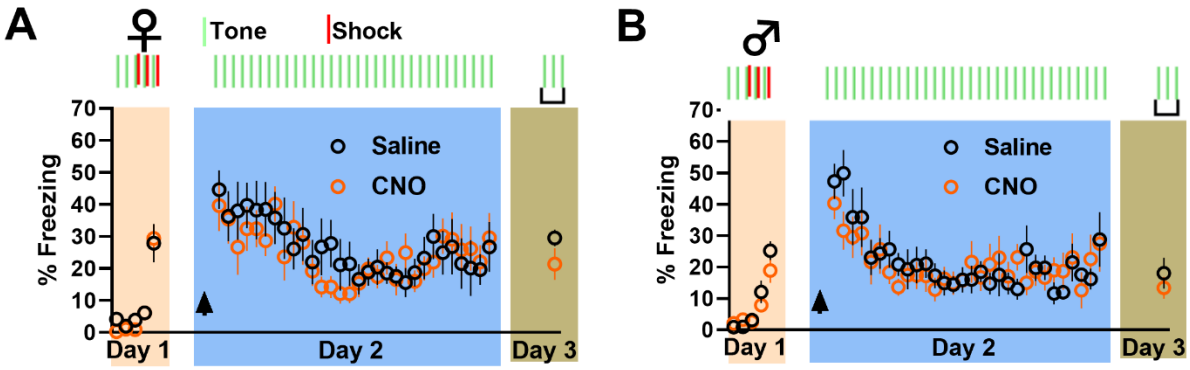
A
♀
Tone
Shock
% Freezing
70
60
50
40
30
20
10
0
Saline
CNO
Day 1
Day 2
Day 3
B
♂
% Freezing
70
60
50
40
30
20
10
0
Saline
CNO
Day 1
Day 2
Day 3

Figure S7

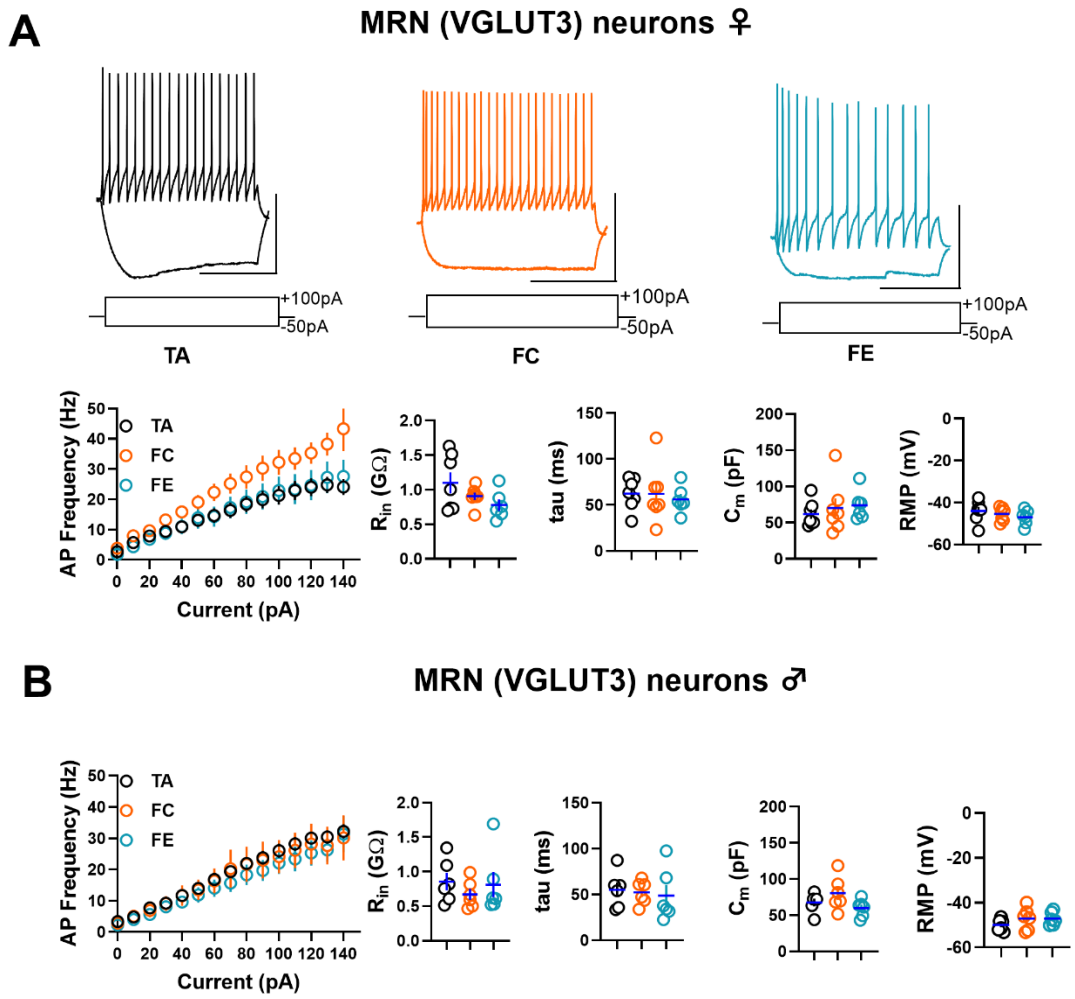
A
MRN (VGLUT3) neurons ♀
+100pA
-50pA
TA
FC
FE
AP Frequency (Hz)
Current (pA)
TA
FC
FE
R_{in} (GΩ)
tau (ms)
C_m (pF)
RMP (mV)
B
MRN (VGLUT3) neurons ♂
AP Frequency (Hz)
Current (pA)
TA
FC
FE
R_{in} (GΩ)
tau (ms)
C_m (pF)
RMP (mV)

Figure S8

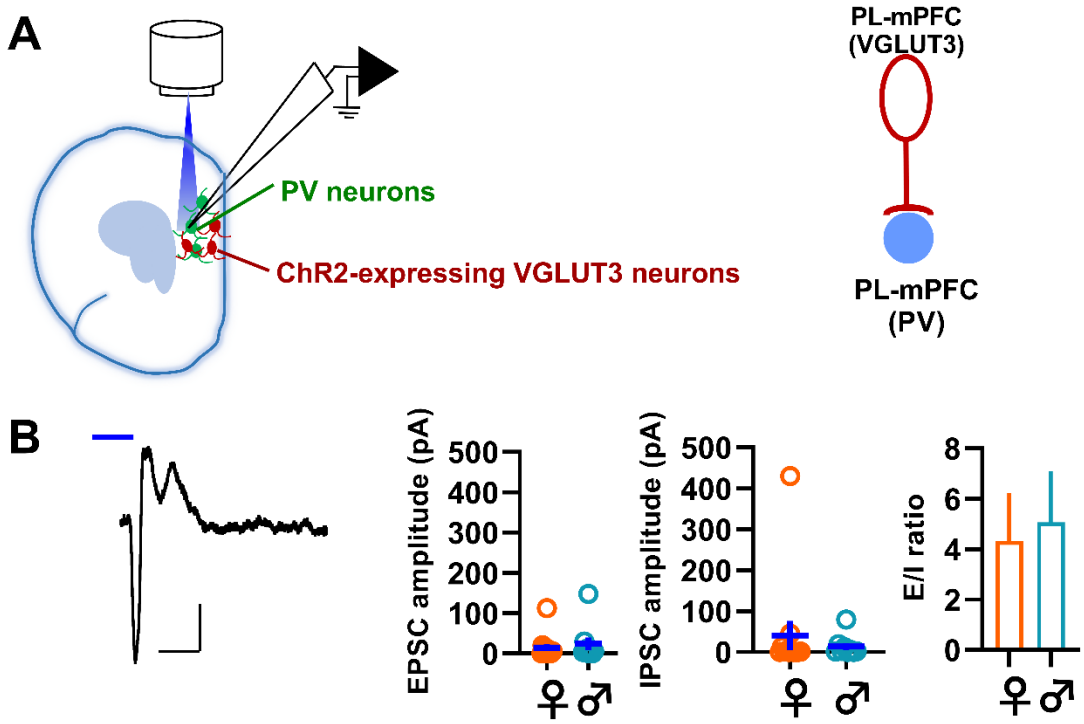
A
PV neurons
ChR2-expressing VGLUT3 neurons
PL-mPFC
(VGLUT3)
PL-mPFC
(PV)
B
EPSC amplitude (pA)
500
400
300
200
100
0
IPSC amplitude (pA)
500
400
300
200
100
0
E/I ratio
8
6
4
2
0
♀
♂